Reply to comments (comments in cursive with our reply below)

1. Replies to comments made by Daout and Dini

a) The day of maximum subsidence cannot be associated with the day of maximum temperature as it is perfectly known with in-situ ground monitoring and permafrost models that the active layer temperature does not follow a diffusive model but is mainly controlled by the Stefan equations (Riseborough, 1996). In other words, the subsidence has been shown to continue, at lower rates, well after the day of maximum temperature, until the temperature falls below zero. In situ-measurements (eg. Gruber et al., 2019 and many others) image this seasonal pattern, which can differ slightly from the Stefan model prediction depending on the moisture content, the snow coverage, the vegetation cover… In addition, the thawing of the ice-rich layers, together with the thaw settlement, can be delayed by few months from the freezing onset. For instance, Liu et al. (2017) document changes in active-layer thickness for the Tien Shan and show with their detailed time/depth graphs that complete active-layer refreezing at depth commonly takes place around the end of the year. Therefore, the lag time between the day of maximum air temperature and the day of maximum subsidence is not a statement from Daout et al., 2017 but a fact.

We agree with your statement, that the lag time between maximum air temperature and maximum subsidence is a widely accepted fact, rather than a new statement made by Daout et al. (2017). We changed our manuscript accordingly, to make sure that this is clear to the reader.

b) The freezing onset is at first order controlled by the time at which surface ground temperatures drop below zero. Amplitude and timing of deformation are then controlled by the water/ice availability and the amount of excess ice in the ground (e.g Daout et al., 2017, Dini et al., 2019). It is, therefore, wrong to draw direct links between the observed deformation and the active layer thickness because the active layer does not follow a purely diffusive model and its behaviour in response to freeze-thaw is associated with the ability of the soil to retain water (grain size, mineralogy..) and the soil thickness.

The approach of Li et al., (2015) to determine the active layer thickness (ALT) from the lag time between maximum air temperature and maximum subsidence is very simplistic, especially as it does not consider variations in the ground moisture content. We therefore removed the section about the calculation of the ALT in this draft of our manuscript.

c) The absence of lag between the day of maximum air temperature and the day of maximum subsidence is most likely linked to a misinterpretation of uncorrected tropospheric delays which is instead attributed by the authors to freeze/thaw related processes. This is also supported by the clear correlation at high-frequency (i.e. well localised patterns following topography) and large scale between the seasonal amplitude and the topography (e.g Fig. 5). As Dini et al., 2019 (Remote Sensing of Environment) show, the attempt to remove atmospheric effects with the use of filters on the time series does not completely remove the layered atmosphere effects. For this reason, Dini et al. show that unless the interferograms are corrected before the time series generation, it is important to apply further corrections, such as those that use atmospheric models and/or empirical corrections generated by looking at the signal-topography correlation. In the aforementioned work, there are plenty of examples taken from a large scale study that indicate the important effects of such corrections and that show the atmospheric dominated seasonal cycles before applying such corrections. The authors do say that they perform a linear spatial trend correction to mitigate for *that, however it is not very clear what this involves and the homogenous timings of maximum subsidence look suspicious for non-atmospheric processes.*

We do not agree with the statement that we misinterpreted the tropospheric delays as freeze-thaw related processes. The reasoning of Daout and Dini to assume this to be the case is (1) the seasonal patterns shown by us follow topographic structures and (2) the correlation between the amplitude of the seasonal patterns and topography. They also ask for clarification on our linear spatial trend correction, which we will answer in (3).

(1) In our opinion Daout and Dini do not take into account, that we separated seasonal freeze-thaw related processes into two different models: the freeze-thaw model in flat areas / valleys and the seasonal sliding model on slopes (described in sections 4.4 and 4.5 respectively). It may therefore seem like our seasonal freeze-thaw related processes follow topographic structures when looking at only one of these models.

(2) If the seasonal pattern we observe in our data was caused by tropospheric delay and not ground deformation, then we would expect to see a correlation between the strength (i.e. the amplitude) of this seasonal signal and the elevation. This has been shown for example by Dong et al. (2019) or Dini et al. (2019). This is not the case in our data (Fig. 1 below). We selected not only one reference point but instead 50 – 90 (Section 4.2), which should also help to reduce the effect of tropospheric delay on our results.

(3) For linear spatial trend correction of the Qugaqie basin we used only regions we expect to be relatively stable on a multiannual scale (i.e. flat and not in immediate contact with water bodies or glaciers). We then determined the linear correlation of their multiannual surface velocity and their elevation. The resulting linear trend (R^2 = 0.12 for ascending and R^2 = 0.38 for descending) was then removed from all ascending and descending data points.

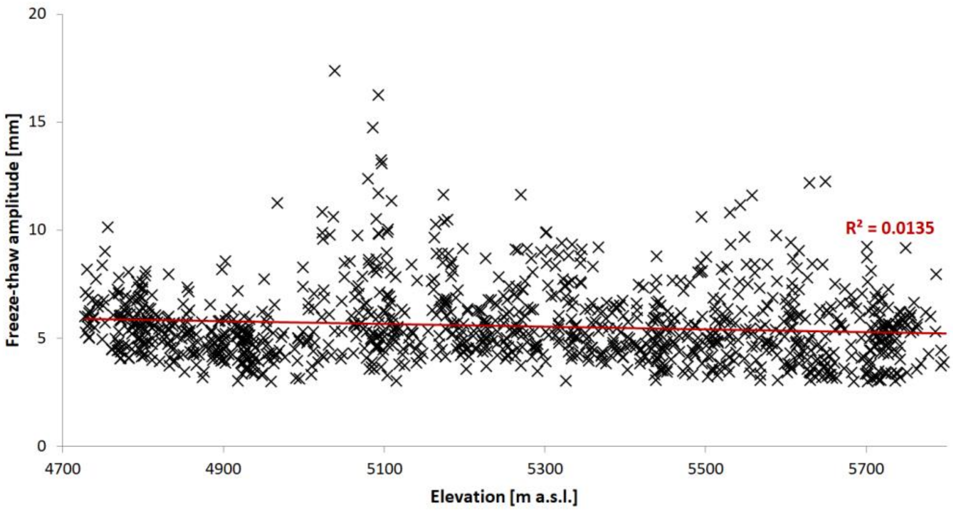

Fig. 1: Diagram of 1000 randomly selected data points (normalized for the lower frequency at higher elevations) showing the relationship between the amplitude of the seasonal signal and elevation.

d) Frost heave/thaw settlement is primarily caused by the formation/thawing of excess ice (these depending on water content and porosity of the soil), especially through ice lenses formation *(segregation ice) in frost-susceptible materials (silt, fine sand, loess) with high water content. Permafrost acts as an impermeable layer that retains the soilmoisture and isolates the active-layer from the deeper ground temperature gradient. Freeze/thaw cycles are therefore mainly detectable in permafrost regions, where the soil contains enough ice/water content to produce thaw settlements higher than 0.5- 1cm. In addition, it is evident that the point of change from subsidence to heave around October/November shown in Daout et al., 2017 relates to delayed thawing at depth (see comment 1), followed by heave as a consequence of the freezing and increasingly cold temperatures penetrating at depth until complete refreezing causes a period of winter inactivity. Also, large-scale models (e.g Qin et al., 2017, Gruber et al., 2012) have described the north-western part of the Tibetan plateau, studied in Daout et al., 2017, as a cold and continuous permafrost region with mean annual ground temperature below -5_C. Daout et al., 2017 can only describe permafrost related process and it is, therefore, unreasonable to think that the observed thaw settlement effects could be associated to freeze/thaw processes in non-permafrost areas.*

We changed the section in question, as Daout and Dini point out correctly, that the comparison drawn in our manuscript is not appropriate here.

e) The article that the authors incorrectly cite (rock glaciers velocities in Bhutan were analysed in Dini et al. 2019 published in RSE, not Dini et al., 2019 published in Engineering Geology) does indeed talk about rock glaciers velocities as they are projected on the steepest slope gradient. The method of assuming that for slope processes (i.e. landslides and rock glaciers) the velocity can be approximated to the steepest gradient is, in fact, quite well established. The authors present in this article a method to calculate a coefficient (correctly citing Notti et al., 2012) which was in fact generated in full by Notti et al. (2012). This is what is also applied in Dini et al. (2019, RSE). Citing from Dini et al., 2019: "If the displacement vector is assumed to be oriented downslope along the maximum gradient, which is a generally acceptable first assumption for gravitational slope movements, then it is possible to estimate the percentage of displacement detectable in the LOS (Notti et al., 2012) and thus to estimate a downslope velocity closer to the true velocity." In addition to this, Dini et al. (2019) looked for decorrelation over rock glaciers in their SBAS results. As the velocities were projected on the maximum gradient and clear decorrelation corresponding to a rock glacier throughout the area of study was not found, it seems fair to state that the relatively slow movements observed over rock glaciers are real (at least over the observation period) and not an effect of misinterpretation of the InSAR results. In addition, the reason why Dini et al. 2019 have not analysed the potential of seasonal accelerations and deceleration of rock glacier movements is due to the temporal sampling of ENVISAT and ALOS, which is on average of 90 days, and therefore completely unsuitable to look at seasonal velocity variations.

We agree that the publication Dini et al. (2019) in "Remote Sensing Environment" is a more suitable citation and we changed the sections in question accordingly.

2. Replies to referee comment 1

Short comments referring to individual words or very minor changes are not listed here but we followed the suggestions of the referee and adopted all the suggested changes.

a) Please be more precise regarding the selection of the temporal and geometrical baselines. Which are minimum and maximum time intervals included in the analysis? As far as I know the Sentinel-1 baseline tube is consistently kept very small so that spatial decorrelation should not be an issue. Did you really exclude interferograms based on the spatial baseline?

The temporal baselines of our interferograms are 12 to 60 days for the Niyaqu basin and 12 to 72 and 12 to 96 days for the Qugaqie basin ascending and descending orbits respectively. Spatial baselines of Sentinel-1 are indeed small compared to other satellite systems and in most cases there are no problems. We discarded a small number of interferograms with relatively long spatial baselines (~200 m) due to poor coherence. We removed the mention of spatial baselines from this section, as the low coherence rather than the spatial baselines of those interferograms were the deciding criteria. We adapted the relevant paragraph in our manuscript to describe the temporal baselines of our data sets and clarify our choice regarding the spatial baselines. We included the connections graphs of both study areas and both orbits in the supplement.

b) What exactly do you mean by "the orbital phase was corrected via a polynomial function"? Which function did you used? How did you determined the coefficients?

Thank you for pointing this out, this paragraph is not correct. It should read: "the orbital phase was removed by subtracting a constant simulated phase from our interferograms. We then estimate a 3rd order polynomial function over flat stable areas and subtract this phase to remove any remaining large scale phase ramps."

c) The paper by Dong et al. (RSE, 2018, https://www.sciencedirect.com/science/article/abs/pii/S003442571930389X) might be of interest in this case and should be possibly included in the reference list.

The publication linked is already part of our reference list.

d) A coherence value of 0.1 is very low, really close to the pure noise level. If most of the interferegrams have in any case a much larger coherence value and the 0.1 threshold was considered to be able to have a spatially consistent solution, then I can understand this choice. But if most of the interferograms have such a low level of coherence, then the results would not be reliable. Please comment.

Data points with coherence values <0.3 represented 4.3 and 8.3 % of the heave-subsidence model in Niyaqu basin and Qugaqie basin respectively. We agree with the assessments of the referees, that a coherence value of 0.1 is too low. We therefore removed data points with coherence values <0.3 from the HSM. All surface displacements models have now a coherence threshold of 0.3. We included coherence maps and maps showing the percentage of interferogram with coherence values above the threshold in the supplement.

e) A drawback of all InSAR time series techniques is the maximum detectable rate of motion, which is related to the possibility to correctly unwrap the phase. A phase cycle at C-band corresponds to 2.8 cm and aliasing are well possible already for half of that value. As mentioned before, the maximum time interval considered in your analyses is missing, but if interferograms spanning several months are considered, than I would expect problems in correctly computing the rate of motion already for few tens of cm/yr (e.g. for three months 2.8Ã°u90_365 = 11.35 cm/yr). If small coherence values are retained, than the most obvious consequence of such an analysis is an underestimation of the rate of motion, in particular for small objects. Please consider if underestimation of the rate of motion for the most rapidly *moving detected landforms cannot be the reason of not seeing a change of motion during the year. In addition, include a statement about what you estimate to be the maximum detectable rate of motion of your analyses.*

Thank you very much for this comment. We will answer be referencing our descending data set of the Qugaqie basin, as it features both the fastest moving landform at up to 8 cm/yr in LOS and then longest temporal baselines (96 days in summer 2016 and 72 days in summer 2017). The coherence of this landform is 0.35 to 0.5. We attached a time series diagram of the cumulative surface displacement at this location (Fig. 2 top). Interferograms of 2018 feature temporal baselines of 12 to 36 days but also do not show seasonal variations in velocity. The longest temporal baseline of 96 days corresponds to a maximum surface velocity of 10.6 cm/yr. It is therefore likely that the velocities of the fastest landforms are being underestimated but not to a huge degree, as the temporal baselines are generally between 12 to 36 days. And only a small number of interferograms in the summer of 2016 and 2017 have long baselines when an underestimation of the displacement is likely. We do not believe that this is the cause of the lack of a seasonal signal in these landforms, as the time series of those landforms do not show an acceleration of their velocity in summer 2018 either. The temporal baselines of summer 2018 are 12-48 days.

This is also corroborated by slightly slower landforms (~4 cm/yr LOS) with similar surface characteristics as the fastest landforms, which also display this motion pattern but are less likely to suffer from an underestimation of the displacement signal. Figure 2 (bottom) displays the cumulative surface displacement of two different landforms with velocities ~4 cm/yr LOS. The landform corresponding to the green line has similar surface characteristics as the fastest landforms and moves at a constant velocity, while the landform corresponding to the red line shows a strong seasonal signal. We updated the relevant paragraphs to show that we considered the possibility of underestimating the displacement signals of the fastest landforms.

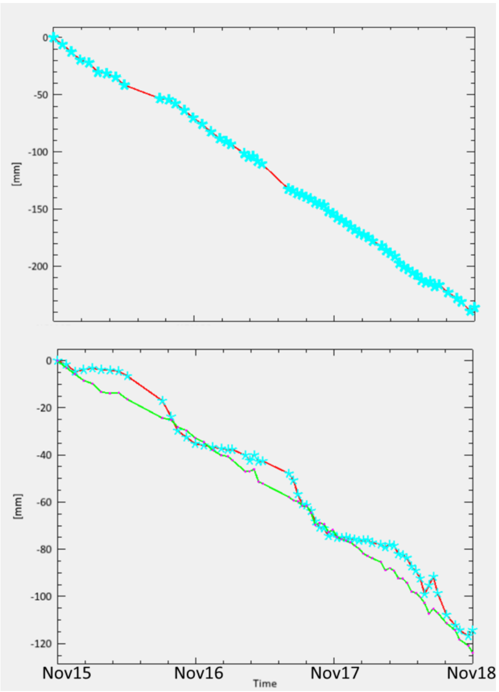

Figure 2: Cumulative LOS displacements of the fastest landform at ~8 cm/yr (top) and two different landforms with velocities of ~4 cm/yr (bottom) in Qugaqie basin in descending orbit.

3. Replies to referee comment 2

Short comments referring to individual words or very minor changes are not listed here but we followed the suggestions of the referee and adopted all the suggested changes.

a) The air temperature (environmental factor) transferred into the ground and varying under and over zero degree leads to phase change of water/ice (process), that leads to frost heave and thaw subsidence (effect). Of course, there is a link between these elements but it is misleading to present InSAR as a technique able to directly measure the freeze/thaw cycles and thermal properties of the ground. In addition, subsidence, even in periglacial environment, can be measured without being necessarily related to thaw. This confusion is present all along the manuscript.

We agree that the terminology we use in the manuscript is at times confusing and does not differentiate well between displacements detected with InSAR and the underlying processes. We adapted the terminology in our manuscript (based on your suggestions) to make this clearer.

b) I would suggest to consider other names for the models and be more clear about their differences from the start (before 4.3). A summary comes at l.333-338, but it is a bit too late. It would be easier to follow if the overall idea is clearly explained just before l.257. FTM name could be changed to heave/subsidence for the reason explained in major comment 1. SSM name is not fully correct: the landforms may have seasonal acceleration/deceleration but do not fully stop creeping. MSM is in general not clear to me: in areas <10deg, what is the difference with FTM? Did you remove the seasonal trend to keep only the multi-annual trend? Is SSM also based on projected results (not clearly stated at l.322-328)? Overall the names are mixing displacement patterns and related processes: maybe easier to choose either process-based names: for ex "heave-subsidence model", "seasonal slope process model", "linear slope process model" or displacement-based names: "vertical cyclic model", "downslope cyclic model", "downslope linear model" (just as examples).

We adapted the descriptions of our three models and their names to make it clearer where each model is applied, what their respective focus is, which processes are covered by each model and go into greater depth to assess their limitations in the discussion as you suggest. We changed FTM (now called heave-subsidence model according to your suggestion) to only cover areas with a slope <10° to make it clearer where each model is applied.

c) The assumption of projection along slopes, if mostly right for landslides and rock glaciers, can be problematic for processes including both downslope and heave/subsidence components (such as solifluction, with displacement normal to slope in winter and vertically down in summer). In addition, it has been documented that these processes can occur on slopes <10 deg (see Matsuoka, 2001). I understand the need to simply but this limitation should at least be acknowledged in the manuscript. Gravity-driven downslope pattern does not necessarily mean permafrost creep, even in periglacial environment. Have you considered the potential presence of rock slope instabilities in these areas? If it sounds possible, you could be a bit more modest in the assumption relating linearity with high ice content (as you state at l.457-462; l.540-543). If not likely in these areas, it has to be stated.

We acknowledge that not discussing rock slope instabilities and solifluction in our manuscript was a grave oversight and we adapted our manuscript to include them as potential causes of the observed displacement. The landforms with a high linear velocities are mainly rock glaciers, protalus ramparts and collapsing moraines. Rock slope instabilities are present throughout the study sites but in those areas we observe mainly seasonally accelerated sliding.

d) Overall, maybe consider to use "downslope-dominated" (or gravity-driven) vs "vertically-dominated" (or freeze/thaw-driven) instead of speaking about linearity/ seasonality. As you write at l.536-538 (too late and too little explained to my opinion), it can "have been misidentified as linearly moving, while actually featuring both the seasonal freeze-thaw cycle prevalent in the valleys and the seasonal sliding pattern of the slopes". A way to check this it to plot the velocity in addition to (or instead of) the cumulated displacement on Fig.6. Fig.6B may look linear but looking at the velocity, I think
you may see variations as well.

We changed Figure 6 of our manuscript to show a time series of the downslope velocity instead of cumulative surface displacement for B and C. We agree that it is important to acknowledge in our manuscript, that the landforms we describe as moving linearly also show variations in their velocities, albeit smaller than other landforms. We now also show the location of the landforms displayed in the time series.

e) Information about several basic data properties and methodological information (important for interpreting the results) is missing: multilooking factor, final spatial resolution, LOS angles, spatial/temporal baseline thresholds, temporal distribution of the initial SAR scenes (baseline plot), map with coherence, map with location of reference areas (in supplementary material for ex).

We added information of the multi-looking factor, spatial resolution and incidence angles to the manuscript. We agree that supplementary material would be very helpful to assess the quality of our data. We therefore added a supplement which contains coherence maps including the locations of the reference points, maps of the interferogram percentage and baseline plots.

f) About ISBAS processing: l.189-190: "... where the coherence is intermittently below the chosen threshold..." and l.198 "... near water bodies, where coherence is very low. We therefore decided to use a very low coherence threshold of 0.1 to increase...": I am not especially known with ISBAS approach, but this sounds quite dangerous to me, especially if you used a threshold of 0.1 in some areas (l.198). Does it mean that you have 25% of interferograms with <0.1 in these areas? Maximizing the coverage also to areas where the results cannot be reliable due e.g. to vegetation or moisture means that some of your interpretation can be based on wrong estimates. At least good to try to explain as much as possible the method, document the uncertainties and acknowledge the potential limitations (in methods and/or in discussion). A coherence map could also be a nice way to document the distribution of these less reliable areas.

We expanded on the discussion regarding the limitations of our data and included coherence maps and interferogram percentage maps in the supplement.

g) Due to this lack of information, it is hard to fully understand the cause of the uplift detected in some flat valley bottoms (l.366 and Fig.3). Looking also at Fig.6A, if you subtract the last and the first acquisitions, you also get a positive trend. Is it really likely that all these locations are affected by sediment accumulation or can it be a bias? I wonder if this cannot be due to low reliability (low coherence) in these areas, especially during the “wet” periods when the ground is subsiding. Or a bias due to the temporal sampling of the initial interferograms? Or atmospheric effect (remaining stratified component)?

One major error source in periglacial environment (during summer) is the impact of ground moisture on the phase (moisture can lead to a biased detection of distance change, up to 10-20% of the wavelength). Good to discuss this. See e.g. references: De Zan et al., 2014; Zwieback et al., 2017.

We changed the paragraphs in question and discuss the possibility of a misinterpretation of soil moisture changes as uplift/sediment accumulation.

h) About DMS: at l.413-414, it is written that there is shift of 11-27 days between ascending/ descending datasets. Why that? 11/27 days is quite a lot, considering that it should in theory document the same thing. Can it be due to a shift of velocity value (problem with the location of the reference points?) or the different LOS incidence angles (different sensitivity to the vertical)? Due to undocumented information about data properties, it is hard to understand the results and fully trust them.

We included information about the incidence angles and added a paragraph to the discussion section regarding the disparity between the DMS of ascending and descending data sets. We also included maps of this disparity in the supplement.

i) DMS 9 days prior to the temperature peak in one of the AOI is presented as "no lag" (l.422, l.427): this is in fact an inverse lag (or lag in the "wrong" direction), which has to be discussed. I would guess this may be due to the distance to the meteorological station: NAMORS station is maybe not representative of this AOI considering that Qugapie has a significantly higher elevation? Did you try to apply an altitude correction? Figure 3: The bottom of the graph E/F is too little explained/exploited in the manuscript. To my opinion, this is maybe the most interesting finding of the study. There is a lack of structure in the Discussion. Consider dividing the Section in three parts, for ex: "Uncertainties/Error source"; "Thaw subsidence / Frost heave cycles";
"Downslope processes".

We reworked the discussion section to explore all mentioned points. We changed the structure to make it easier to follow.

j) The introduction is overall a bit poor. It currently focuses a lot on the Tibetan Plateau, it could benefit for other references to similar kind of studies in others regions of the world. Here an non-exhausive list of ref. that could also contribute to go further with the discussion of your findings: in Alaska: Liu et al., 2010, 2012; Schaefer et al., 2015; in Canada: Short et al., 2014; Rudy et al., 2018; in Greenland: Strozzi et al., 2018; in Svalbard: Rouyet et al., 2019; in Siberia: Antanova et al., 2018.

We updated our manuscript to also present studies other regions besides the Tibetan Plateau in the introduction. We also compare results of these studies to our results in the discussion section.

k) Fig.3: Due to the chosen color scale, it is really hard to see the difference between areas with vertical assumption or those with downslope projection. Also hard to spot the areas affected by subsidence. + Maps C and D are only for Qugaqie basin. Why? + I may have missed sth, but I think there is no mention of the "seasonal sliding coefficient" threshold used to differentiate "linear velocity" and "faster in summer" in map C.

We changed the colour scales to differentiate better between vertical and downslope velocity. We added explanation of the seasonal sliding threshold to the relevant paragraphs and changed the legend of map 3C (now split into two figures and therefore called 7A) to make it clearer. The reason why the slopes of Niyaqu basin are not covered in such great detail compared to Qugaqie basin (not included in Figures 3 and 6 of our original manuscript) is that the spatial coverage of our InSAR data on the periglacial slopes of Niyaqu basin is much poorer. We added a paragraph to our manuscript to explain this. We included the map of the seasonal sliding model of Niyaqu basin in our supplement.

InSAR time series analysis of seasonal surface displacement dynamics on the Tibetan Plateau

Eike Reinosch[1], Johannes Buckel[2], Jie Dong[3], Markus Gerke[1], Jussi Baade[4], Björn Riedel[1]

[1] Institute of Geodesy and Photogrammetry, Technische Universität Braunschweig, Braunschweig, Germany

[2] Institute of Geophysics and extraterrestrial Physics, Technische Universität Braunschweig, Braunschweig, Germany

[3] School of Remote Sensing and Information Engineering, Wuhan University, Wuhan, China

[4] Department of Geography, Friedrich-Schiller-Universität Jena, Jena, Germany

Correspondence to: Eike Reinosch (e.reinosch@tu-braunschweig.de)

~~-~~**Abstract.** Climate change and the associated rise in air temperature have affected the Tibetan Plateau to a significantly stronger degree than the global average over the past decades. This has caused deglaciation, ~~permafrost degradation and~~ increased precipitation~~, heavily changing the water balance of this region. Surface displacement~~ and permafrost degradation. The latter in particular is associated with increased slope instability and an increase in mass-wasting processes~~ are likely~~, which pose a danger to ~~change as the ground continues to warm up and as such it is vital to understand both seasonal and interannual processes dynamics. The Nam Co area is well suited to studying these processes via~~infrastructure in the vicinity. Interferometric Synthetic Aperture Radar (InSAR) ~~time series~~ analysis~~, due to its lack of higher~~ is well suited to study the displacement patterns driven by permafrost processes, as they are on the order of millimeters to decimeters. The Nyainqêntanglha range on the Tibetan Plateau lacks high vegetation and features relatively thin snow cover~~.~~ in winter, allowing for continuous monitoring of those displacements throughout the year. The short revisit time of the Sentinel-1 ~~system~~constellation further reduces the risk of temporal decorrelation, making it possible to produce surface displacement models with good spatial coverage. We created three different surface displacement models to study ~~freeze-thaw processes, seasonal~~ heave and subsidence in the valleys, seasonally accelerated sliding and linear creep~~. Most~~ on the slopes~~ of the area are unstable, with velocities of 8 to 17 mm yr-1, and some landforms reach velocities of up to 18 cm yr-1. The monsoonal climate accelerates those movements during the summer months through high temperatures and heavy rainfall. The fastest moving landforms, some of which have been identified as rock glaciers, do not follow this seasonal pattern of accelerated velocity in summer, instead they follow a linear sliding pattern. It is unclear if this linearity is connected to the ice content in those landforms.~~. Flat regions at Nam Co are mostly stable on a

multiannual scale but some experience subsidence~~, which could be caused by permafrost degradation.~~. We observe a ~~very~~ clear ~~seasonal freeze-thaw~~ cycle of heave and subsidence in the valleys, where ~~thawing and subsequent~~ freezing of the active layer followed by subsequent thawing cause a vertical oscillation of the ground of up to a few centimeters, especially near streams and other water bodies. Most slopes of the area are unstable, with velocities of 8 to 17 mm yr^{-1}. During the summer months surface displacements velocities more than double on most unstable slopes due to freeze-thaw processes driven by higher temperatures and increased precipitation. Specific landforms, most of which have been identified as either rock glaciers, protalus ramparts or collapsing moraines, reach velocities of up to 18 cm yr^{-1}. Their movement does not show a seasonal but a linear pattern indicating that their displacement is predominantly gravity-driven.

1 Introduction

Comment [ER1]: We reworked the Introduction to include more information related to permafrost processes and not only the Tibetan Plateau.

~~The Tibetan Plateau (TP)~~Permafrost describes subsurface material with a temperature of 0 °C or lower for at least two consecutive years (French, 2017). The upper layer of permafrost, referred to as the active layer, freezes and thaws seasonally (Shur et al., 2005). This causes heaving and subsiding of water saturated ground on the order of centimeters due to the volume change associated with the ice-water phase transition. The amplitude of this heaving and subsiding cycle is dependent on the water content of the active layer and the material of the ground (Matsuoka et al., 2003). On permafrost slopes the freezing and thawing of the active layer reduces slope stability (Zhang and Michalowski, 2015) and might create solifluction lobes (Matsuoka et al., 2001). Further examples of creeping landforms associated with permafrost are rock glaciers (Haeberli et al., 2006) and protalus ramparts (Whalley and Azizi, 2003). Approximately 40 % of the Tibetan Plateau (TP) is considered permafrost and 56 % seasonally frozen ground (Zou et al., 2017). Permafrost is vulnerable to climate change (Schuur et al., 2015) and it has been shown, that climate warming may accelerate permafrost related creeping and sliding (Daanen et al., 2012).

The TP has been the object of many studies focusing on climate change over the past decades, especially since it has become known, that its temperature has risen significantly faster than the global average with a rate of 0.~~025~~25°C ~~yr^{-1}~~per decade (Yao et al., 2000). This issue is exacerbated by the importance of the TP as a source of fresh water for large parts of greater Asia (Messerli et al., 2004). The TP is often referred to as the “Third Pole”, as it carries the largest volume of frozen fresh water after the North- and South-Pole. The rising temperature, ~~however,~~ has led to deglaciation at rates of~~-~~ over 0.2 % yr^{-1} (Ye et al., 2017) and permafrost degradation (Wu et al., 2010) throughout the plateau, increasing the river runoff by 5.5 % (Yao et al., 2007). Glaciers and their retreat are very well documented on the TP, as they can be assessed using optical satellite data with high accuracy (e.g. Bolch et al., 2010). Permafrost features, such as rock~~-~~ glaciers or buried ice lenses, are ~~significantly~~ harder to quantify using optical remote sensing due to their ~~debris cover.~~relatively slow motion and often smaller size than glaciers (Kääb, 2008). This has led to a severe lack of inventories documenting these permafrost features, despite their importance as water storages (Jones et al., 2019~~). Other studies have employed~~) and the vulnerability of rock glaciers to climate warming (Müller et al., 2016).

Permafrost related displacement processes, such as slope instability and the creeping of rock glaciers, can be monitored with terrestrial measurement techniques like laser scanners (e.g. Bauer et al., 2003) and studied through the collection of in-situ subsurface data (e.g. Kneisel et al., 2014). These techniques are generally labor intensive, require access to the often remote study sites and provide only sparse spatial coverage. Satellite-based remote sensing does not require access to the study sites and provides large spatial coverage, making it a valuable tool for the study of permafrost related displacements. The displacements vary from a few centimeters (heave and subsidence of the active layer) to decimeters or meters per year (creep of rock glaciers) and are therefore often too small to be studied with optical satellite techniques (Kääb, 2008). Cloud cover may inhibit the collection of continuous optical time series data (Joshi et al., 2016). However, satellites emitting microwaves, like the Sentinel-1 constellation launched by ESA in 2014, make the large scale study of these displacements possible through Interferometric Synthetic Aperture Radar (InSAR) techniques ~~to study permafrost features (e.g. Daout et al., 2017; Dini et al., 2019; Eriksen et al. 2017).~~. InSAR analysis is an active remote sensing technique, which exploits phase changes of backscattered microwaves to determine relative surface displacements taking place between two or more acquisition dates (Osmanoğlu et al., 2016). Other studies have employed InSAR techniques to study permafrost related processes on the TP (Li et al., 2015; Daout et al., 2017), north-western Bhutan (Dini et al., 2019), Norway (Eriksen et al. 2017), Svalbard (Rouyet et al., 2019) and Siberia (Antonova et al., 2018). Both seasonal ~~displacement~~ processes, such as the heave and subsidence ~~and subsequent uplift~~ of ~~thawing and~~ freezing and thawing ground, and multiannual ~~motion~~ processes, like ~~the~~ creep of periglacial landforms, ~~can be~~have been studied. However, interpreting InSAR data can be challenging and often a number of assumptions have to be made. InSAR ~~models~~results provide only motion towards the satellite or away from it, not absolute ground displacement. It is therefore very difficult to accurately assess ground motion, without making assumptions about its actual direction. Unlike optical satellites, which observe the earth from a vertical Line-Of-Sight (LOS), SAR satellites are side-looking and observe the earth ~~at an angle.~~obliquely. In the case of Sentinel-1 this angle varies between 33 and 43° from the vertical (Yagüe-Martínez et al., 2016). SAR satellites are generally right-looking, meaning the microwaves are emitted to the right of the satellite. Due to the polar orbit, this causes the ~~60~~ microwaves to be emitted in a near-east direction while the satellite is ascending and in a near-west direction during descending data acquisitions. The high elevation of the TP brings both advantages and disadvantages to InSAR application. High altitudes can be problematic due to artifacts caused by atmospheric delay (Li et al., 2012), while the lack of high and dense vegetation reduces the risk of decorrelation, which would otherwise lead to poor phase stability, so-called coherence.

This paper presents the results of an analysis of ground movement in the permafrost prone area of the eastern and southern shores of Nam Co based on three to four year time series of Sentinel-1 acquisitions. We identify the various surface processes driving surface displacement~~The high elevation of the TP brings both advantages and disadvantages to InSAR application. High altitudes can be problematic due to artifacts caused by atmospheric delay (Li et al., 2012), while the lack of high and dense vegetation reduces the risk of decorrelation, which would otherwise lead to poor coherence. Coherence is a measure of phase stability and is often used to represent the quality of an interferogram and to determine which pixels will be processed further (Crosetto et al., 2016). A~~

~~problem encountered by many studies investigating periglacial landscapes with InSAR techniques is heavy snow cover during the winter months (e.g. Eriksen et al., 2017), often leading to a complete loss of coherence.~~ ~~This is not a problem in our study sites at Lake Nam Co. In fact, we found that coherence is highest in winter, which we attribute to a stable frozen ground without growing vegetation.~~

~~This paper identifies the various surface displacement processes taking place~~ around Nam Co on the southern TP and evaluates their potential causes. It is vital to understand these displacement patterns and to compare our results to similar studies, as the TP ~~reacts heterogeneously to climate change. Some lakes on the TP show a rising lake level, while others show stable or even falling lake levels (Mügler et al., 2010; Jiang et al., 2017). By assessing land surface displacements processes at Nam Co, we gain further information about the local situation, which allows us to set this region into a more accurate context compared to other regions of the TP.~~has been shown to react heterogeneously to climate change (Song et al., 2014). To that end we developed multiple surface displacement models, analyzing geomorphological processes in the valleys and on the mountain slopes on both a seasonal and a multiannual scale. ~~Furthermore we evaluate our hypothesis to predict if the creep of a periglacial landform is driven by its high ice content by differentiating between linear and seasonal motion patterns. This hypothesis is based on the assumption, that a high ice content within the landform could facilitate significant creep throughout the year, leading to a linear motion pattern, while landforms without ice show no motion during periods when the ground is frozen, hence following a seasonal motion pattern.~~

2 Study Area

The Nam Co is the second largest lake of the TP (Zhou et al., 2013), with a catchment covering an area of 10,789 km², 2018 km² of which is the lake's own surface area (Zhang et al., 2017). The proximity to Lhasa, its accessibility and the presence of the ~~scientific research station NAMORS (Fig.~~ Nam Co Monitoring and Research Station for Multisphere Interactions CAS (NAMORS, Fig. 1), have made it a prime location to study the effects of climate change on the TP. The current lake level lies at 4726 m a.s.l. (Jiang et al., 2017) but it has featured a rising trend of approximately 0.3 m yr^{-1} over the past decades (Kropáček et al., 2012; Lei et al., 2013). ~~To the north and west the endorheic catchment borders on the catchments of smaller lakes, such as Renco and Bamu Co.~~ The eastern and southern borders of the catchment are defined by the ~~eastern and western~~ Nyainqêntanglha mountain ~~ranges respectively. They feature~~range with elevations of up to 7162 m a.s.l. ~~and are partially~~ The highest parts are glaciated (Bolch et al., 2010), while most other areas are considered to be in the periglacial ~~area~~zone (Keil et al., 2010; Li et al., 2014~~), while their highest reaches are glaciated (Bolch et al., 2010). ~~).

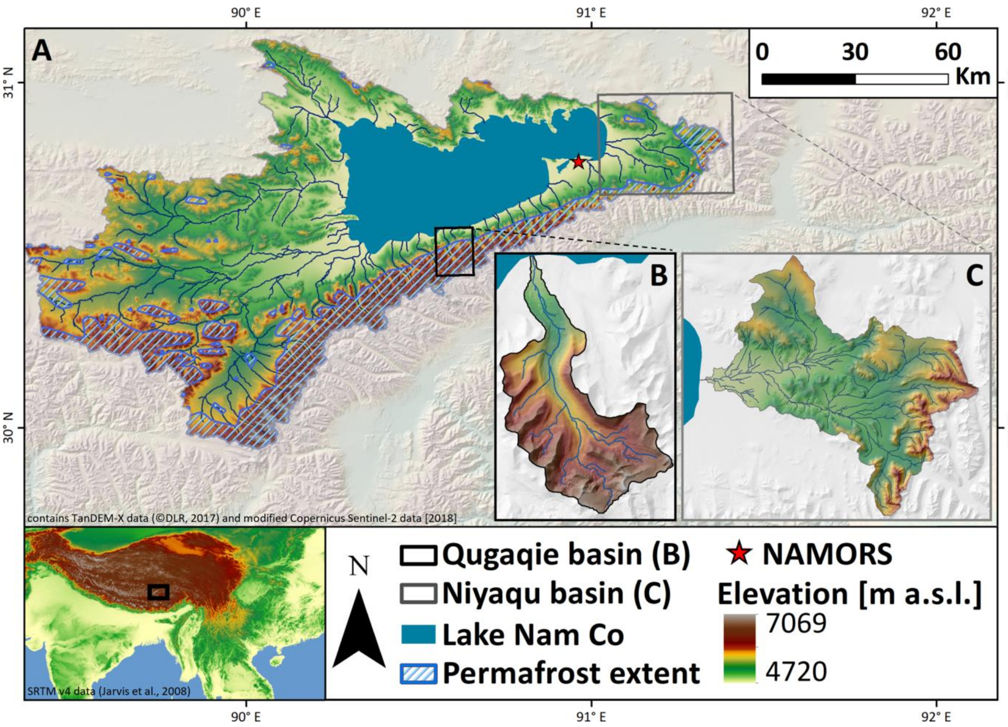

Fig. 1: *Overview map of the Nam Co catchment* ***(A)*** *including the locations of the NAMORS research station and the two main study areas: Qugaqie basin* ***(B)*** *and Niyaqu basin* ***(C)****. Elevation data is based ~~is~~ on SRTM v4 (Jarvis et al., 2008) and TanDEM-X 0.4" DEM (©DLR, 2017). Permafrost extent according to Zou et al. (2017) and lake extent based on the Normalized Difference Water Index (NDWI) of Sentinel-2 optical imagery (©Copernicus Sentinel data 2018, processed by ESA).*

The climate at the Nam Co is dominated by the Indian Monsoon in summer and the Westerlies in winter (Yao et al., 2013). The former brings warm moist air from the south, providing 250 to 450 mm of rainfall from June to September and accounting for approximately 80% of the annual precipitation (NAMORS, 2018; see Fig. 1A). The Westerlies maintain semi-arid to arid conditions during the rest of the year. The snow cover is relatively sparse in winter, due to low precipitation outside of the monsoon season. The vegetation consists primarily of alpine steppe (Li, 2018), with ~~higher~~high vegetation, such as shrubs and trees, being almost completely absent. The sparse snow cover and the lack of high vegetation make this region a prime study site for ~~periglacial~~surface displacement processes using InSAR technology. Wang et al. (2017) used a combination of InSAR and optical satellite data to map rock glaciers in the northern Tien Shan of China, where the winters are similarly dry. The risk of temporal decorrelation, i.e. the loss of data coverage due to ~~a strong~~considerable change of physical surface characteristics, is~~ significantly~~ lower than in other regions where such processes may be studied, such as Norway (Eriksen et al., 2017) or the Sierra Nevada in the USA (Liu et al., 2013). These regions feature ~~significant~~considerable snow cover during long periods of the year, making ~~consistent~~continuous temporal coverage of fast-moving structures, like rock~~-~~ glaciers, difficult. This is especially a problem for satellites with the shorter X-band (2~~-~~ - 4 cm) or C-band (4~~-~~ - 8 cm) wavelengths, like TerraSAR-X (3.1 cm) and Sentinel-1 (5.6 cm), as they are more susceptible to temporal decorrelation (Crosetto et al., 2016) compared to systems with a longer wavelength such as L-Band (15~~-~~ - 30 cm).

The two areas of interest for this study are the Qugaqie basin (58 km²) within the western Nyainqêntanglha mountain range, south of the Nam Co and the Niyaqu basin (409 km²) at the eastern Nyainqêntanglha mountain range, on the eastern shore of the lake (Fig. 1). ~~Those~~These sub-catchments were chosen, ~~to~~as they represent different levels of glacial impact and the predominant landscapes and their related surface ~~motion~~ processes at Nam Co. The Niyaqu basin represents the majority of Nam Co's catchment with extensive alpine steppe vegetation and wetlands surrounded by hills with little exposed bedrock in the lower regions. The global permafrost map of Zou et al. (2017) suggests that periglacial processes are limited to the higher ~~reaches~~parts of the sub-catchment, at the eastern Nyainqêntanglha mountain range. The Qugaqie basin represents the periglacial landscape of the western Nyainqêntanglha mountain range. 60 % of its area are considered periglacial landforms (Li et al., 2014), some of which are still active in the higher ~~reaches~~parts of the catchment due to their potential ice content, such as rock glaciers. Rock glaciers are steadily creeping ice-rich debris on mountainous slopes associated with permafrost (Haeberli et al., 2006). Other landforms were ~~accumulated through~~shaped by fluvial, glacio-fluvial, glacial and aeolian processes (Keil et al., 2010). The vegetation cover is similar to the Niyaqu basin but with more areas of exposed glacial valley fill and bedrock interspersed in between the vegetated areas. Both the valleys and the slopes are covered by unconsolidated ~~material, mostly coarse gravel and boulders, with some slopes being virtually free of soil and vegetation.~~debris, mostly coarse gravel and boulders, and some slopes in the higher parts are free of soil and vegetation. Steep topography and the presence of warming permafrost are associated with rock slope instabilities, such as rock falls and rock slides (Fischer et al., 2006), making them a likely occurrence throughout Qugaqie basin and in the higher zones of Niyaqu basin. The bedrock consists of sandstone and carbonates in the lower areas of the basins and granodiorite and meta-sedimentary rocks in the higher parts (Kapp et al., 2005, Yu et al., 2019). The main river is fed by hanging valleys, some containing glaciers, as well as the two main glaciers Zhadang and Genpu to the south. The glaciers cover 8.4 % of the basin`s surface area and account for 15 % of its runoff in summer (Li et al., 2014). Two automated weather station and a rain gauge were operated near the ablation zone of the Zhadang Glacier between 2005 and 2010. Daily temperature averages range from approximately -15°C in winter to 3°C in summer in the Qugaqie basin and -10°C to 10°C in the Niyaqu basin (NAMORS 2018; Zhang et al., 2013~~).~~)

3 Data

Comment [ER2]: We added the request information regarding incidence angle, multi-looking factor and temporal baselines.

We use~~ exclusively~~ Sentinel-1 Level-1 single look complex data for all InSAR analysis, both from ascending and descending orbits from the interferometric wide swath mode with a ground resolution of 20 m azimuth and 5 m in range direction (ESA, 2012). We used a multi-looking factor of 4 in range direction and 1 in azimuth direction to achieve a ground resolution of 20 m. Sentinel-1a has been acquiring data since October 2014 and Sentinel-1b since September 2016. We found early data acquisitions of Sentinel-1a to ~~be very unreliable~~produce poor interferograms over the Qugaqie basin, which is why we decided to start our time series analysis of ~~this area~~Qugaqie basin in May and November 2015 for ascending and descending acquisitions respectively. Early data over the Niyaqu basin ~~is more stable~~produces better interferograms, here we start our time series analysis already in December 2014 for both ascending and descending acquisitions. The latest~~ data~~ acquisitions included in the analysis are from November and December 2018. Sentinel-1b data is not available for this region, except for a 3 months period at the end of 2016 in descending orbit. More detailed information about the number of acquisitions and interferograms is shown in Table 1. ~~We carefully analyzed all individual interferograms and excluded those with long temporal or geometric baselines, unwrapping errors and overall low coherence and therefore poor spatial coverage.~~The temporal baselines of interferograms are 12 to 60 days for the Niyaqu basin and 12 to 96 days for the Qugaqie basin. All topographic analysis and processing, including the removal of the topographic phase from the InSAR data was conducted, using the 0.4 arc sec, equal to 12 m at the equator, resolution TanDEM-X DEM (©DLR, 2017). This new and truly global DEM has been acquired in ~~the years~~ 2010 to 2015 using single-pass X-Band SAR interferometry (Zink et al. 2014) and finally released by German Aerospace Agency in 2017. On the global scale the DEM features an absolute error at 90% confidence level of <~~-~~2 m (Wessel et al. 2018). In steep terrain accuracy is ensured by multiple data takes in ascending and descending orbits with varying incidence angles to prevent radar shadows and overlay. In the Niyaqu basin, the number of acquisitions per pixel ranges from 5 to 8, with the majority representing average height estimates based on 6 acquisitions. Here, the mean 1 σ height error is 0.30 m. In the steeper Qugaqie basin the number of acquisitions ranges from 8 to 12, with the majority at 9 acquisitions. Here the mean of the 1 σ height error is 0.35 m.

Table 1: *Sentinel-1 data used for the time series analysis of both study areas.*

Area of interest	orbit	Acquisition period	Acquisitions / interferograms	Temporal baselines	Incidence angle
Niyaqu	ascending~~, track 41~~	2014-12-31 to 2018-12-22	79 / 244	12-60 days	40-42°
Niyaqu	descending~~, track 150~~	2014-12-14 to 2018-11-11	72 / 227	12-60 days	39-41°
Qugaqie	ascending~~, track 41~~	2015-06-05 to 2018-12-22	74 / 278	12-72 days	36-37°
Qugaqie	descending~~, track 150~~	2015-11-15 to 2018-12-29	63 / 257	12-96 days	43°

Inserted Cells

Inserted Cells

4 Methods

4.1 ISBAS Processing

There are many different InSAR techniques capable of time series analysis to determine ~~a region's~~ surface displacement over time. We chose a modified version of the Small BAseline Subset (SBAS) method (Berardino et al., 2002), which we performed with the ENVI SarScape software (©Sarmap SA, 2001-2019). The SBAS method generates interferograms between SAR acquisitions with a short temporal baseline, meaning the time between the acquisitions was short, and stacks them to estimate ~~-~~displacement and velocity over a longer time period. Interferograms are a spatial representation of the phase difference of two SAR acquisitions and can be used to determine the relative surface displacement between them. ~~This~~The phase stability, so-called coherence, is often used to represent the quality of an interferogram and to determine which pixels will be processed further (Crosetto et al., 2016). The modified SBAS approach we employ, referred to as Intermittent SBAS (ISBAS~~) (Sowter et al., 2013; Batson et al., 2015~~), produces ~~a significantly~~an improved spatial coverage by allowing limited interpolation of temporal gaps for areas, where the coherence is intermittently below the chosen threshold (Sowter et al., 2013; Batson et al., ~~-~~2015). This reduces one of the downsides of the original SBAS algorithm, where partially vegetated areas can often not be processed, due to ~~only producing good~~the poor coherence ~~for some interferograms but not~~

~~all.~~induced by vegetation. We chose a coherence threshold of 0.3 for our velocity models with an intermittent value of 0.75 and therefore 75 % of the interferograms need to produce a coherence of at least 0.3 to be considered during unwrapping. These parameters are similar to those used by Sowter et al. (2013) and Bateson et al. (2015) and produce an acceptable compromise of good spatial coverage, while excluding most unreliable data from the unwrapping process. We ~~found that the seasonal freeze-thaw signal is most prominent near water bodies, where~~carefully analyzed all individual interferograms and excluded those with unwrapping errors and overall low coherence ~~is very low. We~~and therefore ~~decided to use a very low coherence threshold of 0.1 to increase~~poor spatial coverage~~ in those areas, only for the analysis of the freeze-thaw cycle for our Freeze-Thaw~~. The Heave-Subsidence Model (~~FTM). Both the Multiannual~~HSM), Linear Velocity Model (~~MVM~~LVM) and the Seasonal ~~Sliding~~Slope process Model (SSM) ~~use a threshold of 0.3. The models~~ are explained in detail in ~~the Sections~~Section 4.3 ~~to 4.5 and~~ including a summary ~~may be found~~ in Table 2.

Comment [ER3]: We changed the names of the models and we changed the heave-subsidence model to use a coherence threshold of 0.3, like the other models, due to the valid criticism of the referees.

The topographic phase was removed from the interferograms with the TanDEM-X 0.4 arcsec resolution DEM (Wessel et al., 2018) and the orbital phase was ~~corrected via a polynomial function prior to unwrapping.~~removed by subtracting a constant simulated phase from our interferograms. We then estimate and subsequently subtracted a 3rd order polynomial function over flat stable areas to remove any remaining large scale phase ramps. To reduce spatial trends connected to the small size of the Qugaqie basin we processed a larger area which also includes the two neighboring catchments during the ISBAS workflow. We used a linear model for all processing and applied a short atmospheric high pass filter of only 100 days, to preserve the seasonal signal for our time series analysis, and a low pass filter of 1200 m.

After performing the ISBAS processing chain, flat areas within Qugaqie basin retained a relatively strong ~~shift~~spatial trend of up to 9 mm yr^{-1} ~~and~~ and 13 mm yr^{-1} ~~in~~ in ascending and descending datasets respectively. ~~Due to the respective correlations with a R^2 of 0.12 and 0.38 between this shift and elevation, we~~

~~concluded that this~~This signal is likely connected to an atmospheric phase delay rather than actual surface ~~motion.~~displacement. We therefore performed a linear spatial trend correction to remove this shift from both ascending and descending datasets. The linear spatial trend was estimated through likely unmoving areas with very low slope of <5° with at least 200 m distance to water bodies (based on NDWI of Sentinel-2 optical imagery, ©Copernicus Sentinel data 2018, processed by ESA). After these corrections we performed a decomposition of ascending and descending data sets where we assume displacement in the north-south direction to be insignificant, to determine vertical and east-west displacements. We observe insignificant mean east-west velocities of -0.2~~±2.2~~ mm yr^{-1} and -0.9~~±~~ mm yr^{-1} with standard deviations of 2.2 mm yr^{-1} and 2.4 mm yr^{-1} in likely stable areas in Niyaqu and Qugaqie basin respectively~~. The error range of the slope projection can be up to 5 times as high for areas with a very strong coefficient caused by a large difference between the projection direction and the LOS of the satellite~~.

4.2 Selection of reference areas

InSAR products are relative not only to the LOS of the satellite but also to the chosen reference points or areas. It is necessary to select at least one reference to perform the unwrapping process during the InSAR processing chain. Stable GNSS stations are preferred reference points but there are no permanent GNSS stations installed near the study areas. Therefore it is necessary to select the stable reference areas carefully to avoid introducing ~~a false~~an erroneous trend signal into the surface displacement models. The parameters by which those stable reference areas were chosen are:

1.) ~~Only points located~~Whenever possible we selected areas at high ~~elevation,~~elevations far away from the valley floor ~~were considered.~~. The annual heave-subsidence cycle, and the corresponding uplift and subsidence of the ground, is very strongly represented in the highly moisturized ground of the valley floor. Choosing reference points in this environment would remove this annual ground oscillation from the dataset in the valley floor and create an artificial and opposite oscillation pattern in other areas. The ridges of the Nyainqêntanglha mountain ~~ranges on the other hand~~range feature barely any soil and contain ~~significantly~~ less moisture. Freezing and thawing of the ground should therefore cause a less pronounced heave and subsidence oscillation.

2.) The chosen reference points must be ~~unmoving~~stable during the entire ~~time series~~period of observation, as moving reference points would shift the entire velocity model. We compared the results of different reference points in areas where we expect little ~~multiannual velocity~~motion and discarded those that caused a ~~significant~~ shift. As reference areas we chose regions with a low slope, good coherence and no obvious deformation structures, and assume them to be stable in time.

3.) Ideally the reference points are located on ~~unmoving~~stable bedrock. Bedrock has a much smaller porosity than loose sediment or soil and is therefore less prone to ~~strong~~ oscillations forced by freezing and thawing of pore fluid. ~~Unmoving~~Stable bedrock is associated with a high coherence throughout the year, due to its relatively stable backscatter characteristics.

4.) The reference points must be at locations which are represented clearly in 100 % of all interferograms generated during the SBAS processing chain, to ensure that the displacement of all interferograms can be correctly determined relative to those points.

Despite our careful selection of reference points, we cannot be certain, that those areas are in fact stable throughout the entire data acquisition period. We therefore chose to use multiple reference points instead of a single point to produce the surface velocity models. This prevents a single, potentially poorly selected, reference point from invalidating the entire dataset by introducing either a multiannual velocity shift or seasonal displacement signal. The areas of partially exposed bedrock and the mountainous terrain of the Qugaqie basin made the selection of reference points ~~significantly~~ easier compared to the Niyaqu basin, where exposed bedrock is rare. Selecting only points positioned at these optimal locations left us with none near the center of the basins or the lake shore. This caused velocity shifts along the LOS on a millimeter scale in presumably stable flat areas, if they were far away from the reference points. We therefore increased the number of reference points to 90 and 51 in the Qugaqie basin and 92 and 61 in the Niyaqu basin for ascending and descending acquisitions respectively. Maps showing their locations are included in the supplement. The number of reference areas varies between ascending and descending acquisitions, due to differences in coherence, but we chose the same reference areas whenever possible.

4.3 ~~Multiannual~~Surface displacement models

Comment [ER4]: We added a summary of the three models to make it clearer to the reader how they differentiate from each other and where they were applied.

In total we produced three different types of surface displacement models for the Niyaqu and the Qugaqie basin: The Linear Velocity Model (~~MVM)~~ LVM), the Heave-Subsidence Model (HSM) and the Seasonal Slope process Model (SSM). The LVM portrays the mean surface velocity from 2015 to 2018 and does not portray seasonal variations. It describes both valleys and slopes but we make the assumption that displacements are predominantly vertical in areas with slopes <10° and orientated in a downslope direction in steeper areas. The HSM models the heave-subsidence cycle caused by freezing of the active layer in autumn followed by subsequent thawing of the active layer in spring. It covers only areas with slopes <10°, shows only seasonal displacement and assumes that all displacement is vertical. The SSM was created to differentiate between slopes where sliding is accelerated from spring to autumn and areas where sliding takes place throughout the year at a near linear rate. It only covers slopes >10° and assumes that all displacement is orientated in a downslope direction.

Table 2: *Overview of the 3 surface displacement models with information regarding their purpose, displacement patterns and their connections to geomorphological und geological parameters.*

Modeltype	LVM (Linear Velocity Model)	HSM (Heave-Subsidence Model)	SSM (Seasonal Slope process Model)
Purpose	Identify sediment accumulation and permafrost related processes	Provide information about soil freezing properties	Differentiate between seasonal sliding and linear creep
Displacement type	Multiannual linear velocity along the slope or vertical	Seasonal vertical displacement	Seasonal displacement along the slope
Slope	<10°: vertical velocity >10°: along slope velocity	<10°	>10°
Material	Soil, regolith, till, debris and ice	Mainly soil	Regolith, debris and ice
Related Geomorphological processes	Permafrost creep	Heave-subsidence cycles connected to cryoturbation	Solifluction, gelifluction and rock slope instability on seasonally frozen slopes
Associated Landform	Rock glaciers, protalus ramparts and moraines	Hummocky terrain	Debris mantle slopes and lobates

4.3.1 Linear Velocity Model (LVM)

This model portrays the mean annual surface velocity, with different methods applied to regions with a slope >10° and with a slope <10°. Seasonal displacements trends are not present in this model, as we address those in the separate models HSM and SSM. The original ISBAS processing chain (Sect. 4.1) is the same but we applied different methods~~ thereafter~~ to project the LOS results into a more meaningful direction. For areas with a slope <10° we assumed, that displacement would occur mainly in a vertical direction, as the slope would be too small to facilitate significant sliding or creep in most cases~~ (Daanen et al., 2012) and no tectonic processes, which could produce lateral motion, have been documented for this area.~~. Matsuoka (2001) shows that while solifluction has been documented on slopes as low as 2°, most affected areas in mid-latitude to tropical mountains (including the TP) feature slopes >10°. To determine the vertical velocity, we performed a decomposition of ascending and descending time series data. For this process we assume the north-south component of the ~~ground motion~~surface displacement to be zero, which allows us to determine the vertical and east-west ~~component~~components (Eriksen et al., 2017). The vertical component represents our expected surface velocity for flat areas, while the east-west component can be used to assess the error range of the velocity model.

The decomposition method works well for flat regions and slopes with an east or west aspect but does not produce useful data for slopes with a north or south aspect. The Sentinel-1 SAR ~~satellites are~~satellite constellation is quite sensitive to both east-west and vertical surface ~~motion~~displacement but very insensitive to ~~motion~~displacement with a strong north or south component. This is problematic when studying ~~lateral sliding and creeping processes~~displacements with a large horizontal component, as the velocity of ~~areas~~surfaces moving in a northern or southern direction will be either severely underestimated or completely overlooked. We therefore employed a different method for slopes. Areas with a slope >10° were projected in the direction of the steepest slope ~~(after Notti et al., 2014),~~, as most surface displacement is assumed to be caused by sliding processes transporting material parallel to the slope (Fig. 3). We made an exception for areas with ~~a large~~an east-west velocity >10 mm yr^{-1}, as ~~one of~~ our study areas ~~features~~feature a periglacial setting with landforms such as rock glaciers, which move in a downslope direction and may extend into flatter areas. Those areas were projected in a downslope direction, even on slopes <10°. ~~Our method (after~~ This approach (Notti et al., 2014) originated from landslide studies, to produce a more accurate result for a process, where the direction of the moving structure is either known or can be assumed with reasonable certainty. To estimate the downslope velocity, we calculate a downslope coefficient, with values between 0.2 and 1, based on the LOS of the satellite and the aspect and slope of the surface area. The larger the difference between the LOS vector and the vector representing the assumed motion direction, in this case downslope, the smaller and therefore stronger the downslope coefficient becomes. We excluded data points with a strong coefficient if a slope has a strong coefficient in only one LOS but not the other, as a strong coefficient is associated with a larger uncertainty. The maximum strength of ~~this~~the downslope coefficient is set to 0.2 to avoid producing unrealistically large results caused by a coefficient close to zero. We used a smoothed version ~~of the TanDEM-X DEM~~ (90 x 90 m moving mean) of the TanDEM-X DEM to determine the motion direction~~.~~ ~~We~~, as we assume that structures such as rock glaciers and landslides move a larger amount of sediment in a similar direction. Small scale variations of the aspect or slope have a strong impact on the downslope coefficient and would create outliers in the slope projection in areas with high surface roughness. It is important to note, that by projecting LOS velocities along the steepest slope, we not only assume the direction vector, but we also simplify the mechanics to that of a planar slide. In doing so we assume that neither rotational nor compressing processes are involved. This is an obviously unrealistic but necessary simplification, which leads to on overestimation of the downslope velocity. The error range of the slope projection can be up to 5 times higher for areas with a very strong downslope coefficient than the range of ±2.4 mm we determined over flat ground.

~~***Table 2:** Overview of the 3 surface displacement models with information about their purposes, displacement patterns and their connections to geomorphological und geological parameters.*~~

~~**Modeltype**~~	~~**FTM (Freeze-Thaw Model)**~~	~~**SSM (Seasonal Sliding Model)**~~	~~**MSM (Multiannual Velocity Model)**~~
~~**Purpose**~~	~~Provide information about soil freezing properties~~	~~Differentiate between seasonal sliding and linear creep~~	~~Identify sediment accumulation and permafrost related processes~~
~~**Min. Coherence**~~	~~0.1~~	~~0.3~~	~~0.3~~
~~**Displacement type**~~	~~Seasonal vertical displacement~~	~~Seasonal displacement along the slope~~	~~Multiannual linear velocity along the slope~~
~~**Slope**~~	~~Mostly <10°~~	~~>10°~~	~~<10°: vertical velocity >10°: along slope velocity~~
~~**Material**~~	~~Mainly soil~~	~~Regolith, debris and ice~~	~~Soil, regolith, till, debris and ice~~
~~**Related Geomorphological processes**~~	~~Freeze-thaw cycles connected to cryoturbation~~	~~Solifluction and gelifluction on seasonally frozen slopes~~	~~Permafrost creep~~

~~**Associated Landform**~~	~~Hummocky terrain~~	~~Debris slopes and lobates~~	~~Rockglaciers, protalus ramparts and moraines~~

~~**4.4 Freeze-thaw model (FTM)**~~

4.3.2 Heave-Subsidence Model (HSM)

Comment [ER5]: We went into greater detail about the DMS earlier in the manuscript to make it easier for the reader to follow the results and discussion sections.

Prior to analyzing the ~~freeze-thaw~~heave-subsidence amplitude, we projected the LOS displacements from both ascending and descending datasets to vertical displacement. We then removed the linear multiannual trend from the datasets to isolate the seasonal signal. A sum of sine function was estimated for each individual time series. For the amplitude estimation in the Qugaqie basin we used a function with two sine terms and for Niyaqu basin a function with three terms. We identified the sine term representing the annual signal and discarded the other terms. To qualify for further analysis, a time series must ~~produce an annual freeze-thaw amplitude of larger than 3 mm, with a confidence of R^2 larger than 0.5 and a period of 350 to 380 days. Ascending and descending datasets were interpolated to produce mean amplitude results with a ground resolution of 15 x 15 m~~display a heave-subsidence amplitude larger than 3 mm, with an explained variation (R^2) larger than 0.5 and a period of 350 to 380 days. The main results of the HSM are the amplitude of the heave-subsidence cycle and the Day of Maximum Subsidence (DMS). The DMS describes the mean day on which the sine function reaches its lowest. This represents the day on which the soil has subsided to its minimum level due to thawing before beginning to heave again due to freezing. There is a lag time between the maximum air temperature and the DMS which has been documented to be 2 to 4 months on the TP (Li et al., 2015; Daout et al., 2017). The final HSM contains both ascending and descending data. In areas where they overlap we show the mean value of the two. Slopes >10° were excluded from the HSM as these areas are likely to display mainly gravity-driven displacement with a downslope direction and not only vertical heave-subsidence cycles. The seasonal displacement of slopes is covered by the SSM and their multiannual velocity is shown in the LSM instead.

4.~~5~~3.3 Seasonal ~~Sliding~~Slope process Model (SSM)

The average seasonal velocities represent the median summer and median winter velocities over the entire time series. We divided the median summer velocity by the median winter velocity to produce the seasonal sliding coefficient, which represents how fast a surface is moving in summer compared to winter. Our ~~multiannual velocity models~~LVM feature a precision (1 sigma) of around 2.4 mm yr^{-1}.

Time series with median seasonal velocities ~~within the ±~~<2 mm ~~error range~~yr^{-1} were set to ~~either -2 or~~ 2 mm yr^{-1}, to avoid artificially large values when calculating the seasonal sliding coefficient with median seasonal velocities close to 0. This affects 18.1 % of slopes in Niyaqu basin and 4.3 % of slopes in Qugaqie basin. The higher value in the Niyaqu basin is due to the lower overall velocity of slopes in that region and the reduced spatial coverage due to lower coherence in the higher zone where larger velocities occur. A seasonal sliding coefficient of 1.5 represents a 50 % increased summer velocity compared to the winter velocity. We chose this threshold of 1.5 to differentiate between seasonally accelerated slopes and slopes with relatively linear velocity.

5 Results

~~In total we produced three different types of surface displacement models for the Niyaqu and the Qugaqie basin: The Multiannual Velocity Model (MVM), the Freeze-Thaw Model (FTM) and the Seasonal Sliding Model (SSM). The MVM portrays the mean surface velocity from 2015 to 2018. The FTM aims to isolate the seasonal vertical displacement caused by thawing of the active layer in spring followed by subsequent freezing of the active layer in autumn. The SSM was created to differentiate between slopes where sliding takes place primarily from spring to autumn and areas where sliding takes place throughout the year at a linear rate.~~

5.1 ~~MVM:~~ Linear surface velocity derived from LVM

For the ~~MVM~~LVM, we assumed that displacement occurring in areas with slopes <10° are predominantly vertical in direction, as ~~the low slope is insufficient to produce significant lateral velocity. Daanen et al. (2012) observed, that slopes <10° were unable to support permafrost creep in Alaska. Their findings are~~horizontal displacement is rare in these areas. Solifluction may occur on slopes as slow as 2° but mostly affects areas with slope >10° in mid-latitude to tropical mountain areas (Matsuoka 2001). This is corroborated by the east-west velocity produced by our decomposition of ascending and descending data. For the slopes of 0 - 5°, 5 - 10° and 10 - 15° we observe mean east-west velocities of -0.1~~±~~ mm yr^{-1}, -0.6 mm yr^{-1} and -0.6 mm yr^{-1} at standard deviations of 3.0 mm yr^{-1}, ~~-0.6±~~2.9 mm yr^{-1} and ~~-0.6±~~5.0 mm yr^{-1}~~,~~ respectively. The jump in ~~error range~~standard deviation from ~~the~~ 5 - 10° ~~group~~ to ~~the~~ 10 - 15° from ~~±~~3.0 mm yr^{-1} to ~~±~~5.0 mm yr^{-1} suggests that we observe ~~significantly~~considerably more ~~lateral motion~~horizontal displacement in the latter group. This makes the 10° mark a good threshold between the vertical and the downslope projections. For areas with a slope >10° we assumed that the displacement would occur along the steepest slope, driven ~~my~~by gravitational pull (Haeberli et al., 2006~~) and facilitated by the unconsolidated~~). Unconsolidated material and the lack of deep-rooted vegetation in the area (Li et al., 2014~~).~~) facilitate downslope motion.

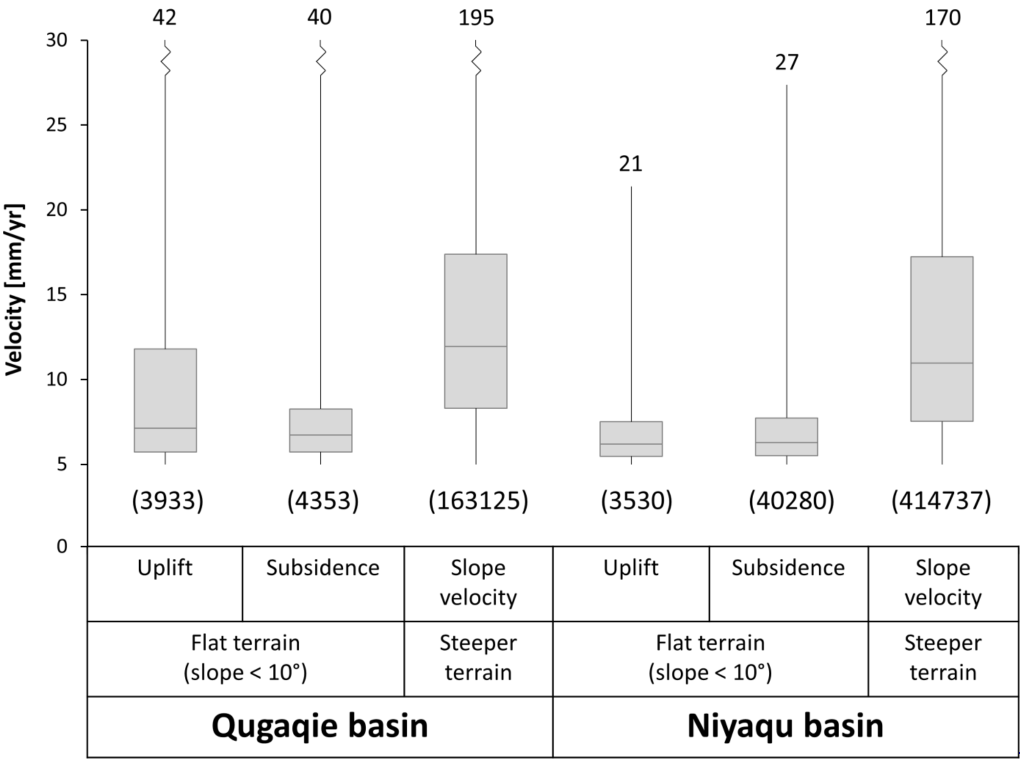

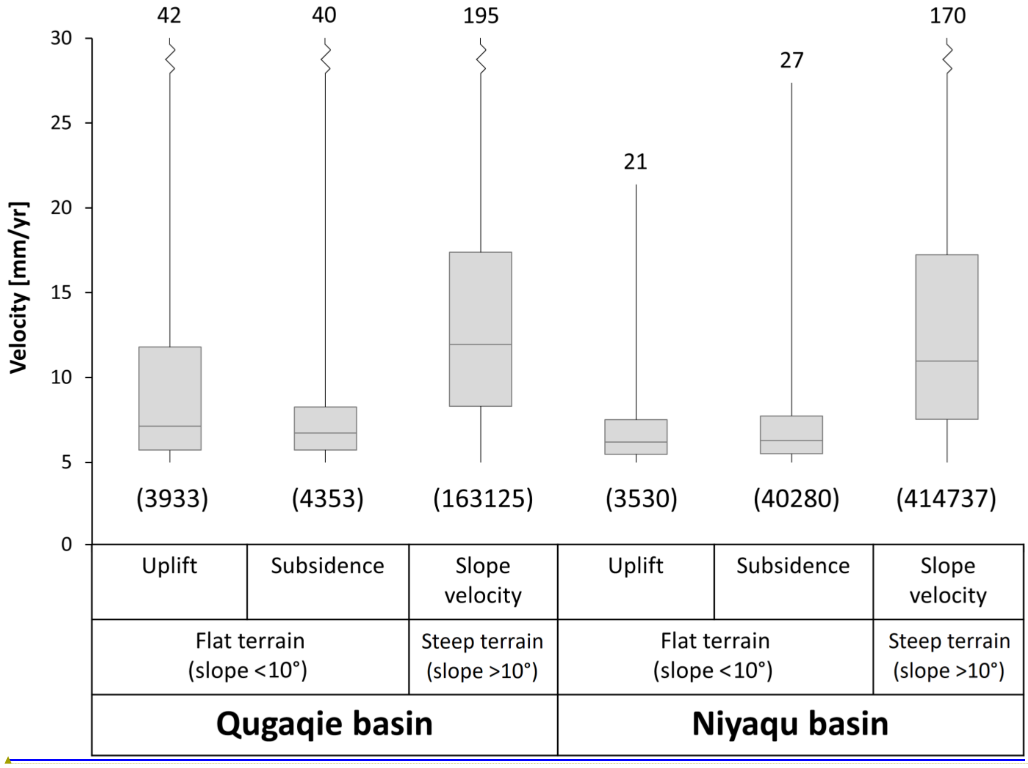

Formatted: Font color: Red

Fig. 2: *Distribution of the mean velocity results of the LVM for unstable flat and steep terrain ~~for the MSV~~ in both study areas. All surface motion in flat areas (slope <10°) was projected into vertical direction (uplift and subsidence) and motion in steeper areas was projected along the direction of the slope. The maximum values are shown above the respective ~~plots~~boxplots and the amount of data points included in each plot is shown in parenthesis below them. Areas with velocities <5 mm* yr^{-1} *are considered stable and are not shown here.*

Spatial data gaps in our InSAR models are caused by layover and shadow effects in mountainous regions or where the coherence was lost due to streams, vegetation, rock falls and glaciers. These data gaps make up 34.7 % in flat and 31.4 % in steep ~~areas~~terrain within the Qugaqie basin and 30.5 % and 36.0 % in the Niyaqu basin. The decomposition of ascending and descending datasets of areas with ~~a~~ flat terrain (slope <10~~º~~°) shows that both basins ~~are~~have relatively stable ~~in~~ flat terrain on a multiannual scale. 53.3 % of ~~the area~~flat areas in the Qugaqie basin and 64.4 % in Niyaqu basin fall within the ±5 mm yr^{-1} velocity group in both vertical and east-west directions. We consider these areas to be stable. In the Quagqie basin 3.3 % of flat areas experience uplift, ~~primarily~~mostly of which are near the main stream, while 2.8 % of flat areas are subsiding. In the Niyaqu basin 0.2 % of flat areas experience uplift and 2.7 % experience subsidence. The remaining flat areas, 5.8 % in the Quagaqie and 2.1 % in the Niyaqui basin, experience minor ~~lateral~~horizontal motion.

__Table 3:__ ~~Quantitative summary~~Summary of ~~our~~ the spatial data coverage of the ~~MVM~~LVM in ~~both~~ the study areas. The ~~shown~~ values represent the percentages compared to all flat or steep ~~areas~~terrain in the respective study area. Incoherent areas display a mean coherence of <0.3. Stable areas ~~move with~~are characterized by multiannual velocities <5 mm yr^{-1} ~~in~~ in all directions, unstable flat areas uplift / subside / move ~~laterally~~horizontally at >5 mm yr^{-1}, steep unstable areas move at >5 mm yr^{-1} downslope and very unstable terrain moves at >30 mm yr^{-1} into the same directions.

	~~Slope~~Terrain	Incoherent	Stable	Unstable	Very unstable
Qugaqie basin	flat (<10°)	34.7	53.3	3.3/2.8/5.8	0.1
	steep (>10°)	31.4	20.9	44.9	2.8
Niyaqu basin	flat (<10°)	30.5	64.4	0.2/2.7/2.1	0.0
	steep (>10°)	36.0	21.1	39.7	3.1

~~Steeper areas, with a slope >10°, are significantly~~Steep terrain is considerably more unstable in both study areas. In the Qugaqie basin only 20.9 % of ~~slopes~~areas in steep terrain are stable, with 2.8 % being very unstable with velocities >30 mm yr^{-1}. In the Niyaqu basin 21.1 % of ~~sloped~~ areas in steep terrain are stable and 3.1 % are very unstable. A summary of the spatial data coverage is shown in Table 3. ~~Most of the low coherence areas would likely be considered unstable as well and would therefore increase the percentage of unstable and very unstable areas.~~ A distribution of the absolute surface velocity results in different regions is shown in Figure ~~2~~3.

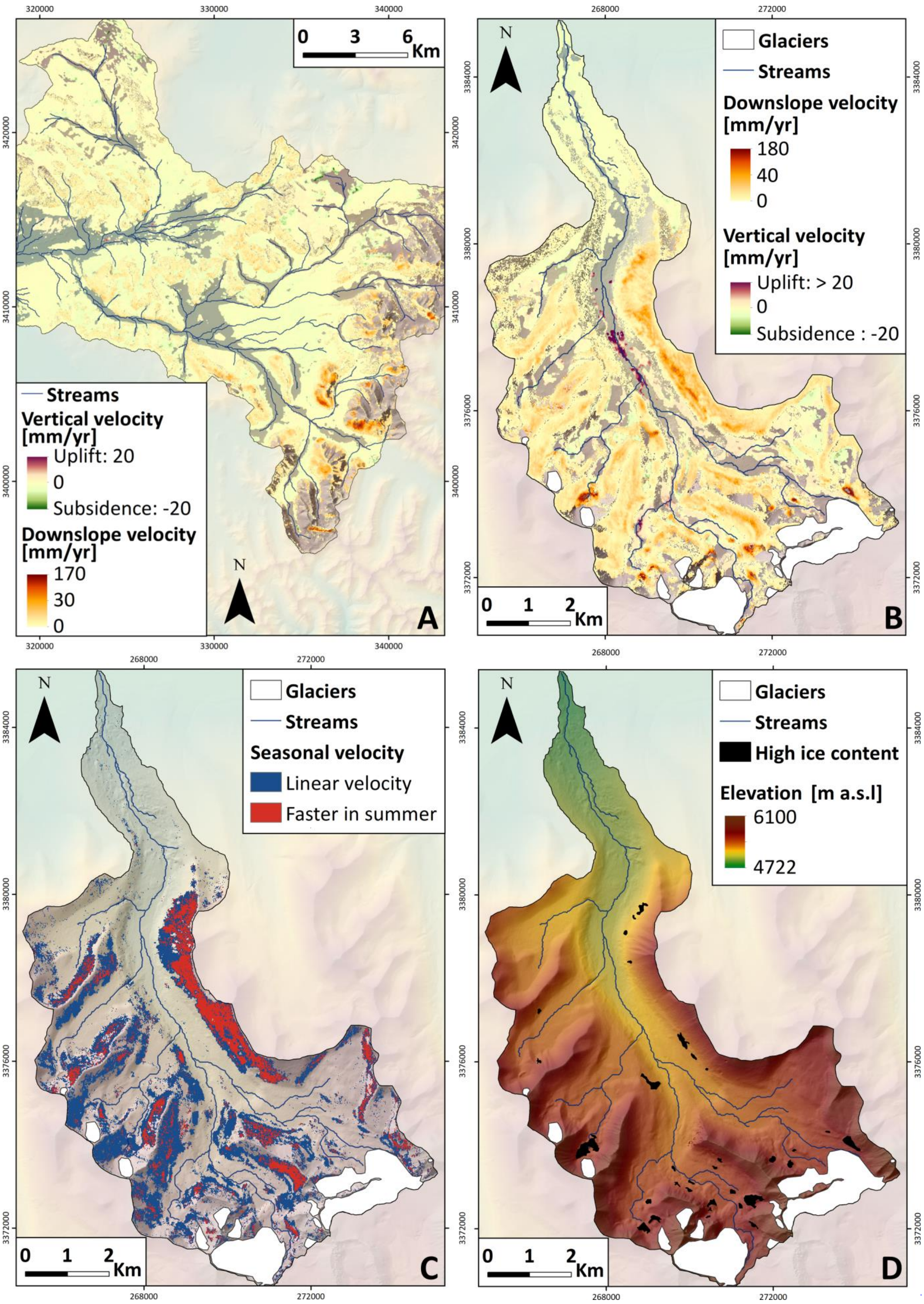
0 3 6 Km
Streams
Vertical velocity [mm/yr]
Uplift: 20
0
Subsidence: -20
Downslope velocity [mm/yr]
170
30
0
A
Glaciers
Streams
Downslope velocity [mm/yr]
180
40
0
Vertical velocity [mm/yr]
Uplift: > 20
0
Subsidence : -20
0 1 2 Km
B
Glaciers
Streams
Seasonal velocity
Linear velocity
Faster in summer
0 1 2 Km
C
Glaciers
Streams
High ice content
Elevation [m a.s.l]
6100
4722
0 1 2 Km
D

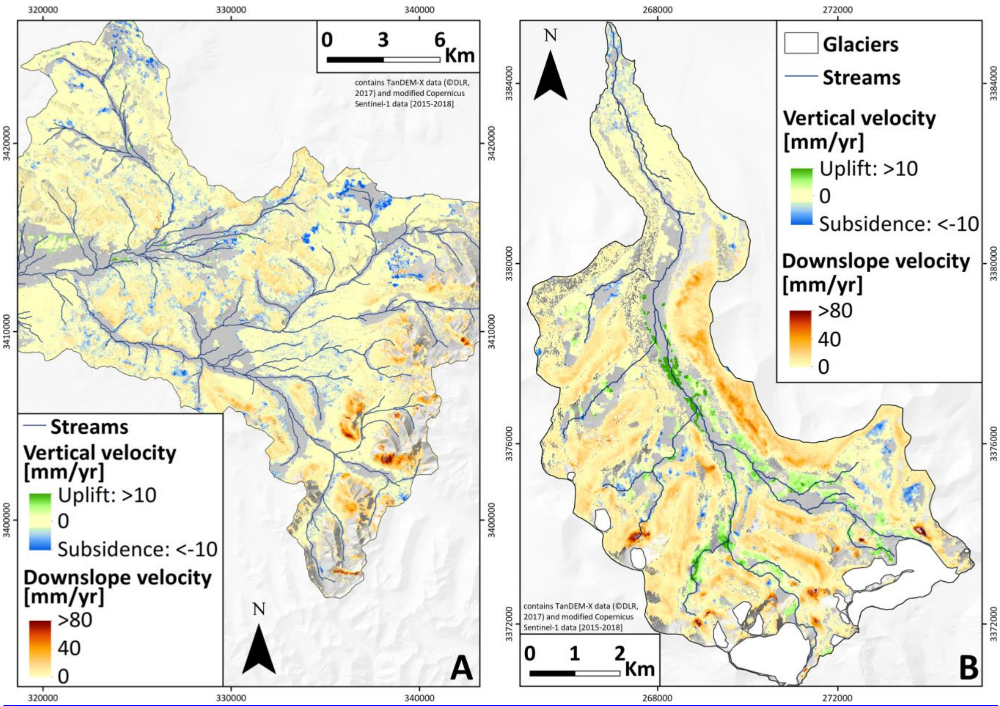

***Fig. 3**: ~~Surface displacement models~~LVM of the relevant parts of the Niyaqu (A) and Qugaqie (B) basins based on Sentinel-1 data ~~(modified~~ (©Copernicus ~~Sentinel-1 data [~~2015-2018~~]~~)) over TanDEM-X DEM (©DLR, 2017). ~~A/B: MSM of Niyaqu/Qugaqie basin, where areas~~Areas with a slope <10° show vertical velocity and steeper slopes show the surface velocity projected along the steepest slope. ~~C: SSM of Qugaqie basin displaying the spatial distribution of linearly moving slopes and those with a more than 50 % faster velocity in summer as compared to winter. Only areas with a slope >10° and a slope velocity >10 mm yr-1 are shown. D: Spatial distribution of clusters where we assume a high ice content based on a high slope velocity with a linear pattern.~~*

Comment [ER6]: We adjusted our colour choices and moved the second half of this figure to the section regarding the seasonal slope process model (now Figure 7).

The coherence in both basins is much reduced in valley ~~areas.~~bottoms. Streams and other water bodies ~~inundate~~affecting as well the soil ~~with~~ moisture~~, creating~~ status of the neighboring land surfaces cause large changes in microwave backscatter properties depending on the season. More extensive vegetation near the valley bottom further reduces the coherence ~~there~~. The coherence is especially low in ~~those areas~~valley bottoms during the spring and the summer monsoon period, when the ground thaws, the surface is inundated by rain water or runoff and biomass production increases. This causes an overall drop in spatial data coverage in ~~valleys~~valley bottoms, as many resolution cells exhibit coherence values below the threshold. Coherence maps of ascending and descending orbit of both study sites are included in the supplement.

~~5.2 FTM: Freeze-thaw amplitude~~

5.2 Heave-subsidence cycle derived from HSM

The seasonal vertical oscillation of the ground due to freezing and thawing of the soil is strongest ~~at~~in the valley bottom, especially near streams, lakes, ponds and, in the case of Qugaqie basin, glaciers~~.~~ (Fig. 5 A/B). In these areas the amplitude of this oscillation can reach up to 19 mm ~~(~~in the Qugaqie basin~~, Fig. 5C)~~ or even 27 mm ~~(~~in the Niyaqu basin~~, Fig. 5A).~~. The ~~day of maximum subsidence (DMS)~~median amplitude error is 1.3 mm in Niyaqu basin and 1.1 mm in Qugaqie basin. The DMS is the day in summer during which the soil has ~~thawed~~subsided to its ~~maximum extent~~minimum level before beginning to ~~freeze~~heave again in autumn (Fig. 5 ~~B~~C/D). In the Qugaqie basin the median DMS is on July ~~12~~19 and in the Niyaqu basin it is on August ~~24~~23 (Fig. 4). Most ~~areas~~data points with ~~freeze-thaw~~heave-subsidence amplitudes of <7 mm reach their day of maximum subsidence in July to August in the Niyaqu basin and May to July in the Qugaqie basin, while areas with larger amplitudes tend to reach theirs in September to October (Fig. 5E/F). ~~This trend~~The median shift error of the sine function modeling the heave-subsidence cycle is ~~more pronounced~~33 days in the Niyaqu basin and 27 days in the Qugaqie basin. We compared the DMS results of ascending and descending datasets and noticed that in both basins the mean DMS of the descending dataset occurs earlier. In the Niyaqu basin the difference between ascending and descending DMS is 27 days and in the Qugaqie basin ~~11 days. For this comparison we only took areas into account with a large density of both ascending and descending data points.~~ 10 days. Maps showing the spatial distribution of this disparity are included in the supplement.

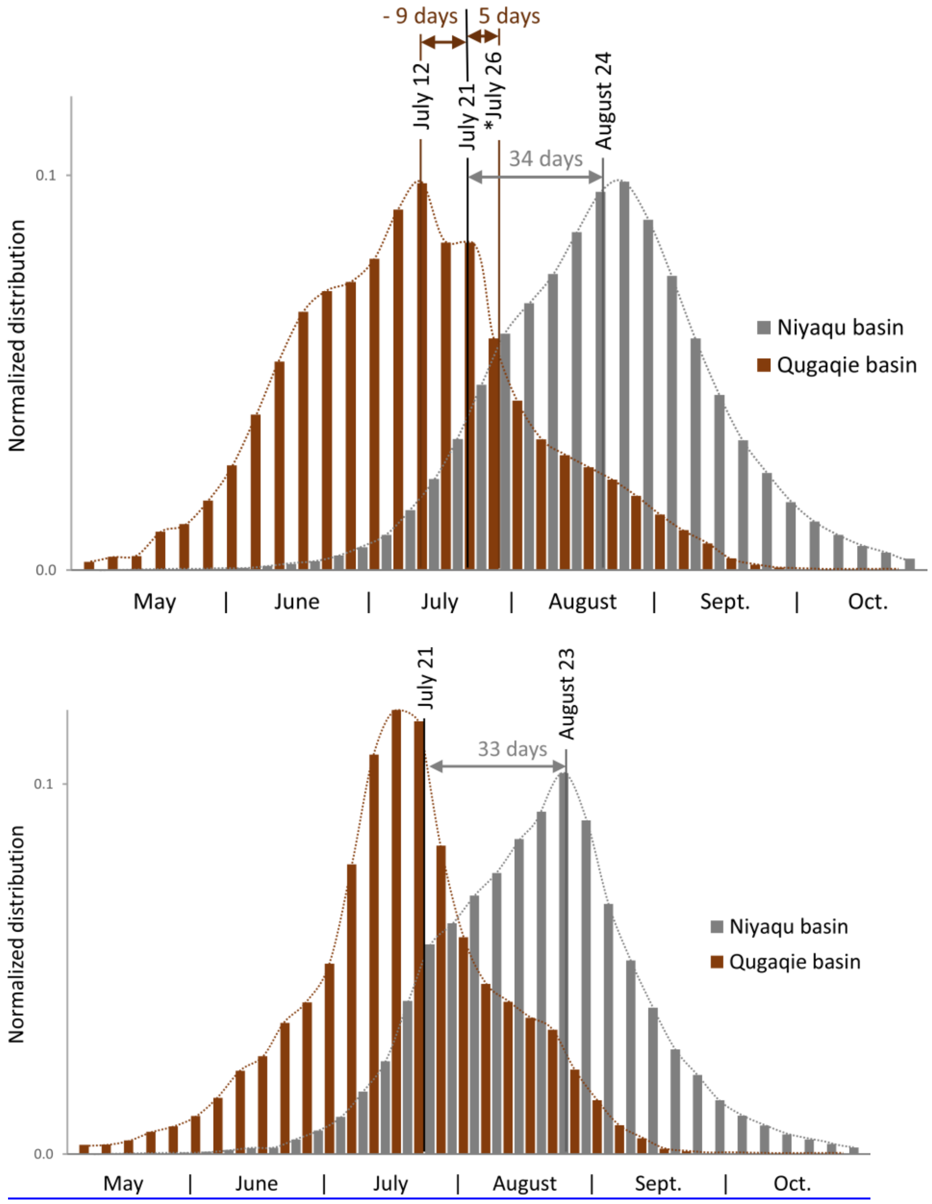

Fig. 4: *Normalized distribution of the thaw-induced ~~day~~Day of ~~maximum subsidence~~Maximum Subsidence (DMS) in the Niyaqu basin (grey) ~~and the Qugaqie (brown) basins and their respective~~ with a median ~~values~~value on August 24 and ~~July 12.~~the Qugaqie basin (brown) with a median value on July 21. The lag time of 33 days between ~~those~~the median ~~values~~value of Niyaqu basin and the day of the mean maximum air temperature ~~are~~ on July 21 (NAMORS, 2018) is also shown. The ~~mean air temperature peak~~median DMS of Qugaqie basin occurs on July ~~21 (NAMORS, 2018),~~19 resulting in ~~a~~ no clear lag time ~~of 34 days in the Niyaqu basin and no lag time in~~.*

Comment [ER7]: The changes in this figure and Fig. 5 are due to our adjustment of the coherence threshold from 0.1 to 0.3.

The freezing and thawing of soil follows the ~~*Qugaqie basin, as*~~ Stefan equation (Riseborough et al., 2008) and there ~~*the median DMS occurs 9 days prior to the mean air temperature peak.*~~

~~Other studies~~ is~~(Li et al., 2015; Daout et al., 2017) have stated that there is often~~ a significant lag time between the day of maximum air temperature and the DMS. This lag time has been studied with InSAR remote sensing techniques both on the northern and the southern TP (Li et al., 2015; Daout et al., 2017). According to the weather data from the NAMORS research station, the air temperature has a mean peak on July 21±1 day from 2010 to 2017. Data from the weather station at the Zhadang glacier (Zhang et al., 2013) shows this mean peak on July 27±5 days for 2010 to 2011~~.~~ (July 19±8 days for the same period at NAMORS). Due to the very short ~~data~~ acquisition period of only two years for the ~~data from this~~Zhadang weather station, we chose the ~~more robust~~eight year data set of the NAMORS for both study areas. This produces a lag time of approximately ~~34~~33 days for Niyaqu basin (Fig. 4, grey), while in the Qugaqie basin the median DMS occurs ~~9~~on July 19, two days ~~ahead of its~~before the maximum air temperature ~~peak~~ on July 21, resulting in no clear lag time (Fig. 4, brown). ~~We used this lag time to determine the active layer thickness (ALT) by assuming the heat transfer to be one-dimensional and the soil to be homogeneous. Our chosen thermal diffusivity is 4x10-7 m^2/s, based on the mean value for frozen soil after Wang et al. (2005), and we followed the heat transfer model of Li et al. (2015). The resulting ALT is 1.3±0.7 m for Niyaqu basin. We did not determine the ALT for Qugaqie basin, as we do not observe a lag time here and the system is therefore likely too complex for this simplified approach.~~

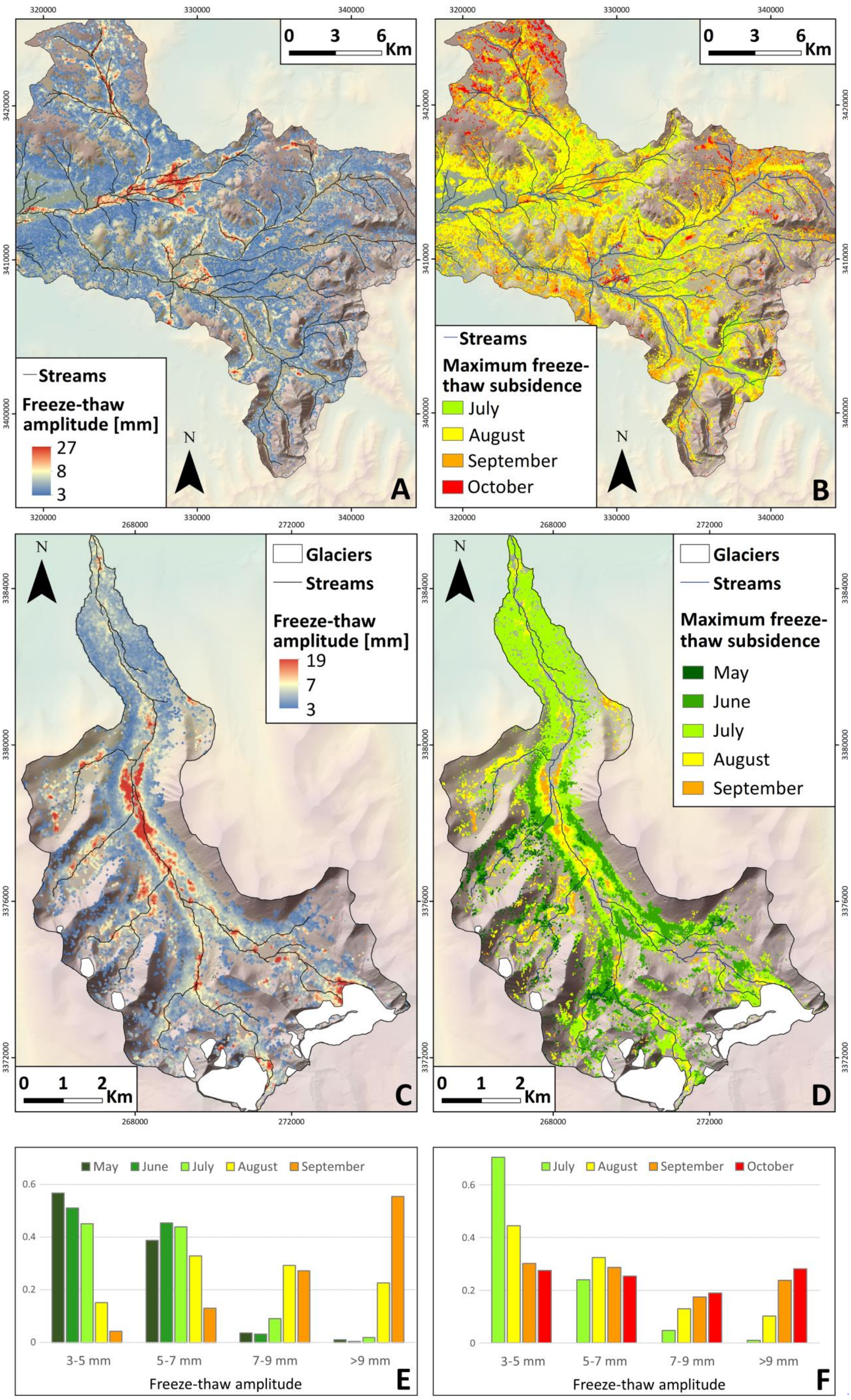

A
B
C
D
E
F
0 3 6 Km
0 1 2 Km
N
Streams
Glaciers
Freeze-thaw amplitude [mm]
27
8
3
19
7
3
Maximum freeze-thaw subsidence
May
June
July
August
September
October
3-5 mm
5-7 mm
7-9 mm
>9 mm
Freeze-thaw amplitude

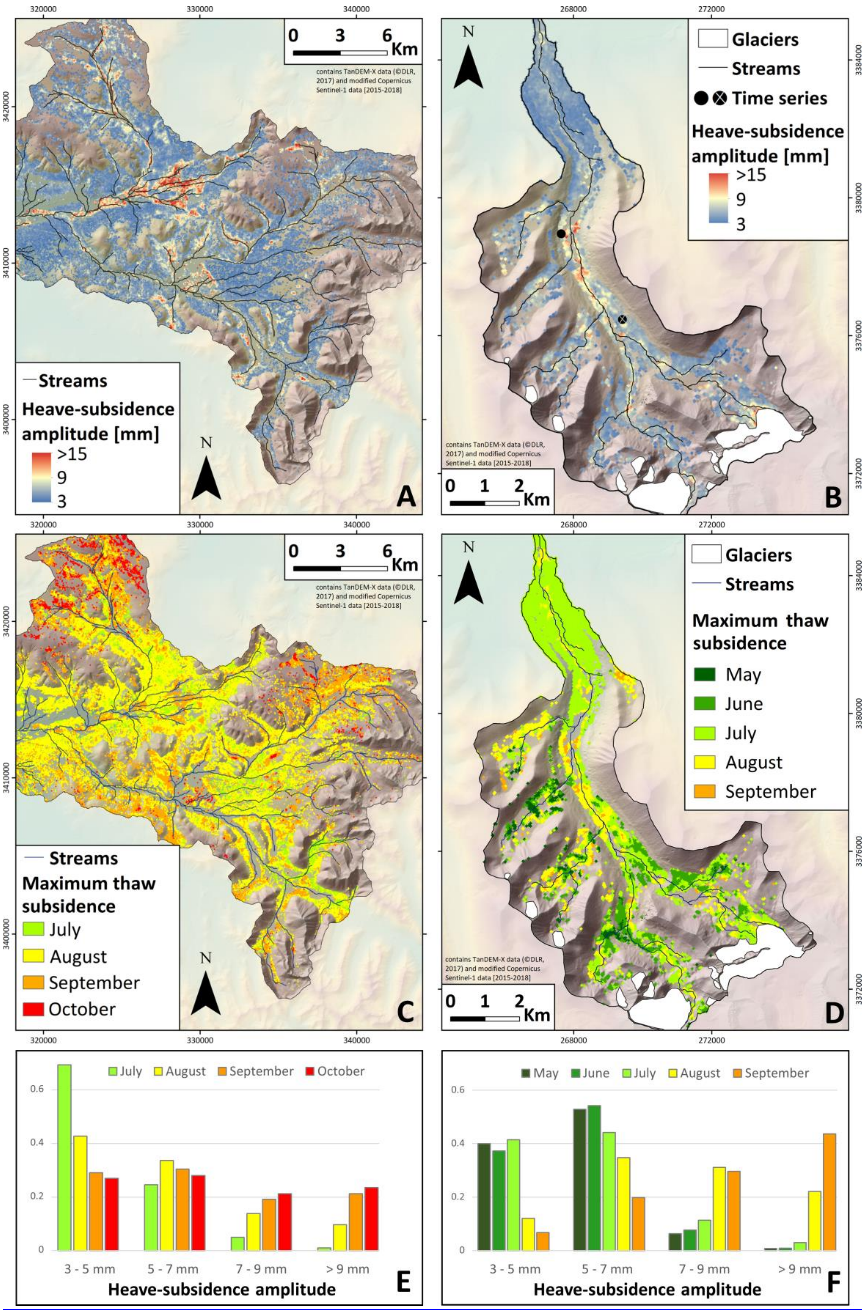

***Fig. 5**: ~~Seasonal freezing and thawing parameters~~Parameters of the HSM (modified Copernicus Sentinel-1 data [2015-2018]) over TanDEM-X DEM (©DLR, 2017). Spatial variations of the mean amplitude (**A/~~C~~B**) and the day of maximum subsidence (**~~B~~C/D**) of the ~~FTM~~HSM within the Niyaqu/Qugaqie basin. The locations of the time series of Figure 6A are displayed as black dots. **E/F:** Normalized distribution of the months in which the ~~freeze-thaw~~heave-subsidence cycle reaches their*

maximum subsidence split up into 4 groups according to their amplitude for the Niyaqu/Qugaqie basin.

5.3 ~~SSM:~~ Seasonally ~~sliding~~accelerating slopes derived from SSM

We identified two distinct seasons, the wet monsoon season in summer and the dry winter season, which have a ~~significant~~clear impact on the displacement data. The former season causes ~~more pronounced~~accelerated ground sliding on many slopes, while the latter ~~arrests~~slows most sliding processes~~.~~ (Fig. 6C). In Niyaqu basin the accelerated displacement pattern of the summer period lasts from May to September and in Qugaqie basin from June to October. The slower winter displacement patterns last from November to March and from December to April respectively. We compared the median summer velocities to the median winter velocities of each time series over the entire ~~time-period. Most debris covered slopes in both basins slide significantly faster during the summer months and some of them, especially in the Qugaqie basin, stop their motion altogether in winter (Fig. 4 C).~~study period. Most soil or debris covered slopes in both basins display accelerated sliding rates of 100 to 300 % towards the end of the summer monsoon. They reach downslope velocities of mostly 50 to 150 mm yr^{-1} during that time. The lower areas of most slopes appear to move at a linear rate. This marks the interface between the heave-subsidence cycle of the valley bottoms and the seasonally accelerated sliding on the slopes. These two seasonal displacement processes (Fig. 6A/C) are both present in those interface areas and often interfere with each other in such a manner, that they appear to move linearly in the SSM.

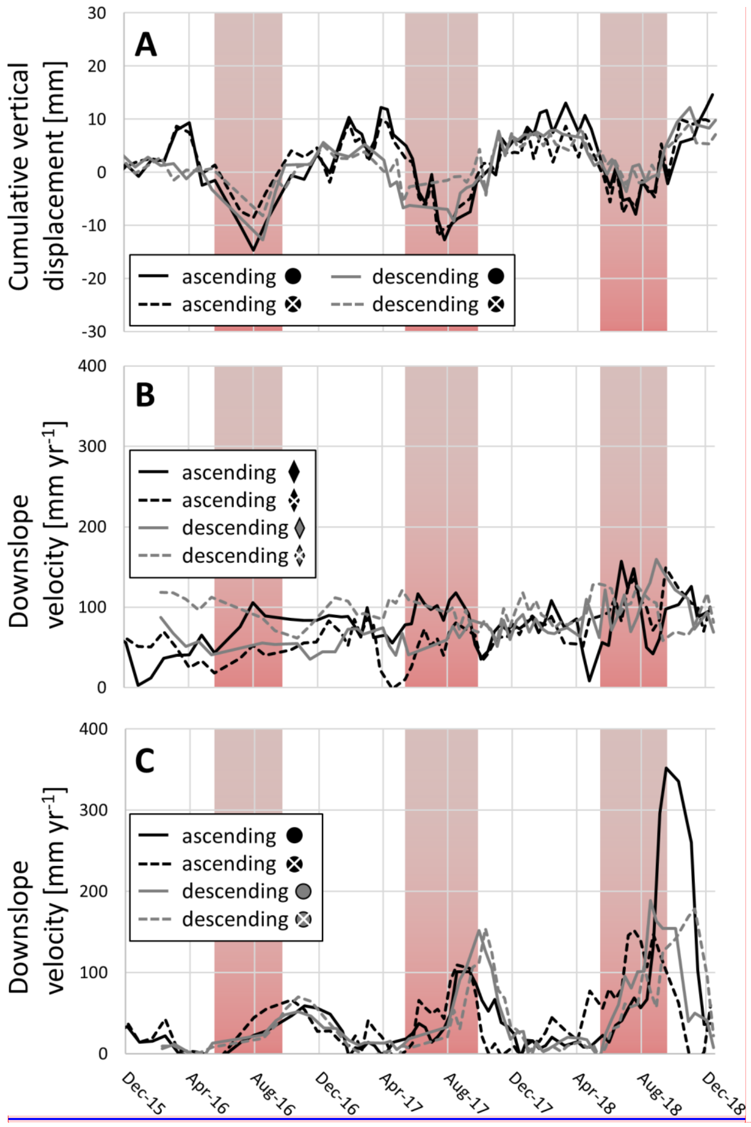

Comment [ER8]: We changed B and C of this figure according to the suggestions of referee 2 to display velocity instead of cumulative displacement.

Fig.

*-**6**: Surface displacement time series of both ascending (black, dashed black) and descending (grey, dashed grey) data of various areas throughout Qugaqie basin highlighting the three seasonal patterns. June to September are shown with a red background as they display the strongest monsoon activity and air temperatures >0 °C (Zhang et al., 2013). **A:** Cumulative vertical displacement showing the seasonal heave-subsidence cycle of the HSM at two locations near the stream of the main valley (black dots in Fig. 5B). **B:** Downslope velocity time series of the four gravity-driven landforms (rhombi in Fig. 7A) with relatively constant velocities (blue areas in Fig. 7A). **C:** Freeze-thaw-driven displacement patterns on four slopes (dots in Fig. 7A) with accelerated displacements in summer and*

comparatively minor displacements in winter (red areas in Fig. 7A). B and C display moving average values of the closest 4 values in time.

In Qugaqie basin and to a lesser extent in the Niyaqu basin, we observe that some of the fastest moving structures creep at a linear rate as opposed to the strong seasonality of most slopes. ~~Their velocity changes very little between~~They do not display a clear acceleration in summer and ~~winter and~~ their multiannual velocity is generally between 30 to 180 mm yr^{-1}~~.~~ (Fig. 6B). We ~~performed a cluster analysis of these structures to identify their distribution throughout the valley and noticed that some of them correspond to periglacial features we~~ identified some of these landforms as rock glaciers or protalus ramparts from optical satellite imagery, field observations and topographic analysis. The motion of these permafrost related ~~structures, such as rock-glaciers and protalus ramparts~~landforms, is driven by an ice matrix in between unconsolidated debris material (Haeberli et al., 2006). Rock glaciers and protalus ramparts represent 36 % of the linearly fast moving landforms in the Qugaqie basin and include the largest and the fastest landforms with this displacement pattern. Other landforms with this displacement pattern are rock slope instabilities (24 %) and collapsing moraines (39 %). We focus our analysis of slope displacements on the Qugaqie basin, due to the considerably better overall coherence and therefore spatial coverage of slopes in the periglacial zone. The maps equivalent to Figure 7 for Niyaqu basin characterized by poor coherence in the periglacial zone can be found in the supplementary material.

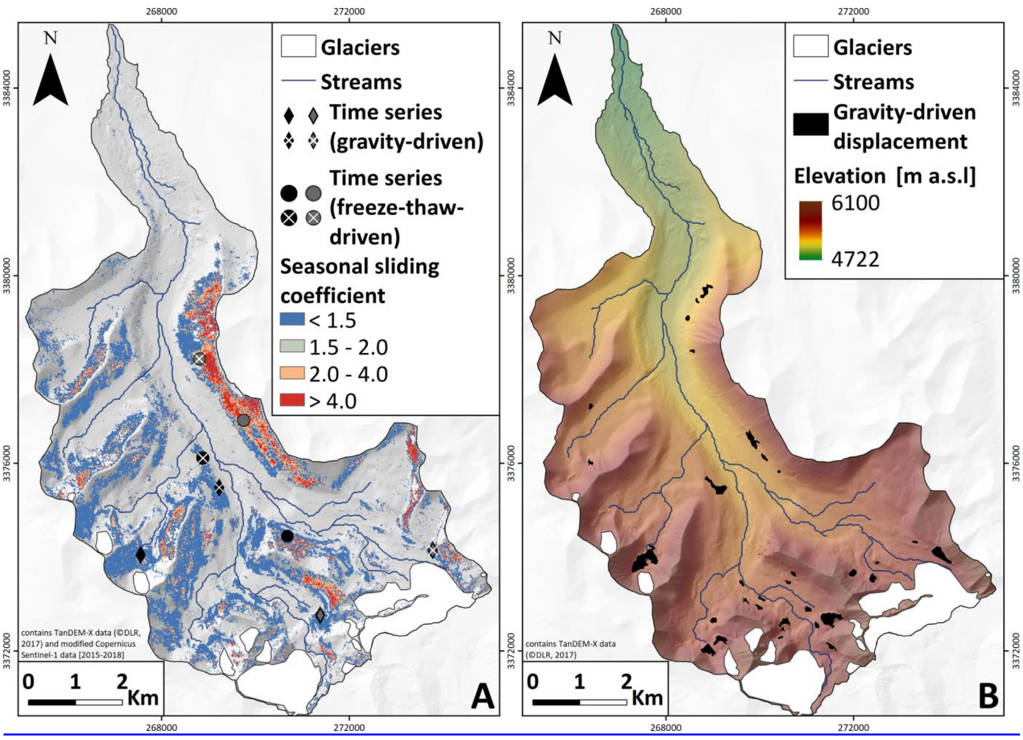

Fig. 7: A: *SSM of Qugaqie basin displaying the spatial distribution of slopes with accelerated surface velocity in summer compared to winter. A seasonal sliding coefficient of 1.5 represents a 50 % increase of the velocity in summer. Only areas with a slope >10° and a slope velocity >10 mm yr^{-1} are shown. The locations of the time series in Figure 6B/C are shown as rhombi/dots.* ***B:*** *Spatial distribution of clusters where we assume displacement to be gravity-driven. These clusters display slope velocities >50 mm yr^{-1} and a seasonal sliding coefficient <1.5.*

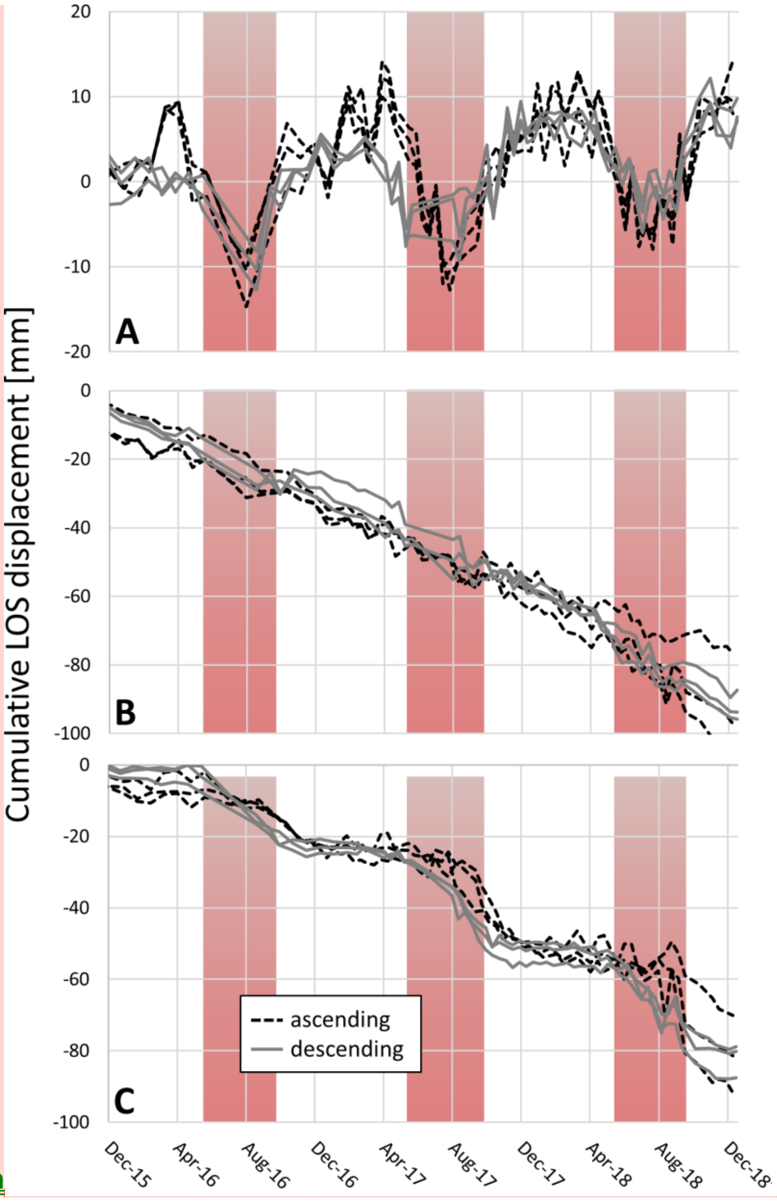

6 Discussion

Comment [ER9]: The discussion section was reworked to go into greater depth regarding the limitations of the models. The structure was changed to make it easier for the reader to understand which part of which model is being discussed.

We created three different models to study both seasonal and multiannual surface displacements and their driving processes in steep and flat terrain at Nam Co. We discuss the multiannual displacements of the LVM and the seasonal displacements of the HSM in flat terrain in Sections 6.1 and 6.2 respectively. Multiannual displacements of the LVM and seasonal displacements of the SSM in steep terrain are discussed in Sections 6.3 and 6.4 respectively.

A ~~*Fig. 6: Cumulative LOS displacement of both ascending (black dashed) and descending (grey) data of various areas throughout Qugaqie basin highlighting the three seasonal patterns. The months with the strongest monsoon activity (June to September) are shown with a red background. A: Seasonal freeze-thaw cycle of the FTM near the stream of the main valley. B: Linear displacement patterns of various structures classified as potentially containing a large amount of ice (blue areas in Fig. 3C). C: Seasonal displacement patterns of various slopes highlighted by the SSM with large displacements in summer and comparatively minor displacements in winter (red areas in Fig. 3C).*~~

~~6 Discussion~~

~~Zhao et al. (2016) demonstrated, that using a linear model to process regions with cyclical freeze-thaw~~problem encountered by many studies investigating periglacial landscapes with InSAR techniques is heavy snow cover during the winter months (e.g. Eriksen et al., 2017), often leading to a complete loss of coherence. In our study sites we found that coherence is highest in winter. This is likely due to the arid winter climate leading to little snow cover and stable soil moisture, low surface displacements on slopes due to frozen ground and lack of vegetation growth. Zhao et al. ~~mechanisms leads to an overestimation of the displacement signal. We could not confirm their findings in our study areas. We therefore decided to use a linear model for all processing, as the quadratic model produced almost identical results and the cubic model produced unreliable results with poor spatial coverage. Both the Niyaqu and the Qugaqie basin are relatively stable in flat areas~~(2016) demonstrated, that using a linear model to process regions with cyclical heave-subsidence mechanisms leads to an overestimation of the displacement signal. We could not confirm their findings in our study areas. We therefore decided to use a linear model for all processing, as the quadratic model produced almost identical results and the cubic model produced unreliable results with poor spatial coverage.

For both our seasonal and our multiannual surface displacement models we distinguish between flat terrain with slopes <10° where we assume all displacement to be mainly vertical and steep terrain with slopes >10° where we assume displacement to occur in a downslope direction. We chose this threshold based on the decomposition of ascending and descending results, which shows a considerable increase of horizontal velocities on slopes >10° compared to flatter areas. While this simplification is necessary and mostly accurate for our study areas, it leads to inaccuracies especially in areas with slopes of 5 to 15° where displacements can occur in both vertical and downslope directions.

6.1 Multiannual displacements in flat terrain

Flat terrain~~on a multiannual scale but show a strong seasonal signal in the same areas (Fig. 6A). It is unlikely that this signal is induced by seasonal atmospheric effects, as the amplitude would likely correlate to some degree with relative elevation to the reference points (Dong et al., 2019), which is not the case for our data. The most likely explanation is, that this signal displays the freeze-thaw cycle of moist soil. Others observed very similar signals over permafrost areas and seasonally frozen ground on the northern TP (Daout et al., 2017) and in Dangxiong county on the southern side of the Nyainqêntanglha range (Li et al., 2015). We estimated a sine function for every individual time series to determine the spatial distribution of this signal. This is only an approximation of this signal and not a true representation of its parameters as it does not follow the trend of a sine curve perfectly. Nonetheless we consider it a valid if imperfect approach. We could not identify any significant difference in the freeze-thaw cycle between areas where permafrost is likely to be present and areas where the ground is only seasonally frozen. We therefore disagree with similar studies (Daout et al, 2017; Li et al., 2015) that associated this process with permafrost. The amplitude, the day of maximum thaw subsidence and the active layer thickness of those studies agree well with our results from the Niyaqu basin. In the Qugaqie basin this is not the case for the latter two. Li et al. (2015) observe an increasing lag time of up to 98 days in mountainous areas, which they attributed to thicker permafrost and colder surroundings. A small amount of their data points fall within the Qugaqie basin, showing lag times of 50 to 90 days. We observe a significantly shorter lag time, with most areas in this basin reaching their maximum subsidence ahead of the maximum air temperature by a few days to weeks (Fig. 4). It is possible, that the difference between their results and ours is reflecting actual changes to the lag time between their dataset of 2007 to 2011 and ours of 2015 to 2018 but the point density of their data within Qugaqie basin is too low to draw reliable conclusions. The absence of a lag time in the Qugaqie basin in our results could possibly be explained by the small size of the basin. Its small size may let the basin react much quicker to environmental changes, such as dropping temperatures, compared to a larger basin like the Niyaqu. It is also possible, that the thawing process in the Qugaqie basin is not as closely linked to air temperature and other parameters, such as precipitation and glacial meltwater, play a larger role.~~

~~Most regions with small slopes~~ throughout both basins can be considered relatively stable with mean vertical and east-west velocities within ±5 mm yr^{-1}. Some ~~regions~~areas in ~~valleys~~valley bottoms show uplift rates of up to 40 mm yr^{-1} (Qugaqie basin, Fig. 3B) and 21 mm yr^{-1} (Niyaqu basin, Fig. 3A). ~~These regions are likely experiencing some form of sediment accumulation through the nearby streams.~~ A possible explanation is that seasonal variations in the soil moisture content were misidentified as surface displacement. The melt water and high monsoon precipitation increases the soil moisture in summer, which can lead to a false interpretation of surface displacement of 10 to 20 % (Zwieback et al., 2017). In our case this would represent 5 to 10 mm per monsoon season for a total of 15 to 30 mm. This is corroborated by the large amplitude of the heave-subsidence model in the same areas, which is associated with a higher potential heave-subsidence amplitude by providing more water during the freezing process (Fort and van Vliet-Lanoe, 2007).

We also observe subsidence rates of up to -12 mm yr^{-1} in Qugaqie basin and -25 mm yr^{-1} in Niyaqu basin. Many of those ~~data points~~pixels are close to streams ~~or other~~and water bodies~~, making fluvial processes the most likely cause. However, approximately~~. Approximately 30 % in the Niyaqu and 60 % in the Qugaqie basin fall into permafrost regions (Zou et al., 2017; Tian et al., 2009~~) further away from water bodies.~~). This makes permafrost degradation a potential driver of this subsidence, as a thinning permafrost layer would result in ~~meltwater~~melt water escaping from the thawing soil. However, longer periods of observation are needed to come up with reliable conclusions.

6.2 Seasonal displacements in flat terrain

Both the Niyaqu and the Qugaqie basin have relative stable flat terrain on a multiannual scale but show a strong seasonal signal in the same areas (Fig. 6A). It is unlikely that this signal is induced by seasonal atmospheric effects, as the amplitude would likely correlate to some degree with relative elevation to the reference points (Dong et al., 2019), which is not the case for our data. The most likely explanation is, that this signal represents the heave-subsidence cycle of freezing and thawing of moist soil. Others observed very similar signals over permafrost areas on the northern TP (Daout et al., 2017) and over seasonally frozen ground in Dangxiong county on the southern side of the Nyainqêntanglha range (Li et al., 2015). The heave-subsidence amplitude of these studies agrees well with our results of mostly 3 to 15 mm in both basins. In similar areas they observe amplitudes of 2.5 to 12 mm and 10 to 25 mm respectively. Comparable studies of permafrost landscapes measured thaw subsidence of predominantly 10 to 70 mm and 2 to 68 mm per thawing season on Spitsbergen Island (Rouyet et al., 2019) and in northern Siberia (Antonova et al., 2018) respectively.

In both of our study sites we observe a relation between the amplitude of the heave-subsidence cycle and the DMS (Fig. 5E/F). Areas with high amplitudes tend to reach the DMS later in the year

(September to October) and areas with small amplitudes tend to reach their DMS earlier (July to August). The lag time between maximum air temperature and DMS is therefore greater for areas with a large heave-subsidence amplitude. Longer lag times have been associated with a deeper active layer when assuming a one-dimensional heat transfer in soils (Li et al., 2015). For our study areas this would imply, that the active layer tends to be deeper near streams and water bodies, as both the heave-subsidence amplitude and the lag time are highest there. This agrees with other studies on active layer thickness, which also observe a deeper active layer in those areas, especially where water bodies remain partially unfrozen in winter (e.g. McKenzie and Voss, 2013).

Other studies observed considerably higher lag times between the highest air temperature and the DMS. They observe lag times of 97 days and 65 days in flat areas (Daout et al., 2017; Li et al., 2015) with longer lag times in mountainous areas, which they attributed to thicker permafrost, colder surroundings and less soil moisture. A small amount of the data points of Li et al. (2015) fall within the Qugaqie basin, showing lag times of 50 to 90 days. In Qugaqie basin we observe no clear median lag time (Fig. 4). It is possible, that the difference between their results and ours is reflecting actual changes to the lag time between their dataset of 2007 to 2011 and ours of 2015 to 2018 but the point density of their data within Qugaqie basin is too low to draw reliable conclusions. We determined the lag time by comparing the DMS to the average maximum air temperature at NAMORS from 2010 to 2017. NAMORS is located at an elevation of 4730 m, which is considerably lower than most valley areas of Qugaqie basin at up to 5600 m. The temperature data acquired by Zhang et al. (2013) within the Qugaqie basin shows a maximum air temperature on July 27, 6 days later than at NAMORS. Their data set covers a period of less than two years and is therefore likely too short for an accurate comparison but it indicates that the maximum air temperature is too similar to that of NAMORS to explain the short lag time. The Qugaqie basin has a short thaw period, with only 80 to 100 days in summer reaching daily air temperatures >0° (Zhang et al., 2013). Together with the presence of permafrost this may explain the short lag time between the maximum air temperature and the DMS. A short thaw period is associated with a thinner active layer (Åkerman and Johansson, 2008) and the cold mountain climate and the permafrost would accelerate the freezing process of the active layer. While this may help to explain the short lag time, it also highlights a major limitation of the model. For the HSM we estimated a sine function for every individual time series to determine the spatial distribution of the heave-subsidence cycle. Areas where this cycle does not follow a sinusoidal pattern are therefore not represented accurately by the HSM. The short thaw period of the Qugaqie basin also shortens the periods of maximum subsidence compared to the periods of maximum heave (Fig. 6A), hence making the heave-subsidence cycle less sinusoidal. Together with the short time series of only 3 to 4 years, this leads to a high shift error of the sine function of 27 days in the Qugaqie basin and 33 days in the Niyaqu basin.

The difference of the DMS between ascending and descending data sets is 10 days in the Qugaqie basin and 27 days in the Niyaqu basin. This is a very high disparity for a displacement with a predominantly vertical direction, which should be represented equally in ascending and descending data sets if the incidence angles are comparable. The difference in incidence angles between the two orbits is 6° over the Qugaqie basin and 1° over the Niyaqu basin. Over the Qugaqie basin the resulting difference in sensitivity to vertical displacement may help to explain the 10 day disparity between ascending and descending data sets but it does not explain the large disparity of 27 days in the Niyaqu basin. The most likely cause of this disparity is the imperfect manner in which the sine curve of the HSM estimates the heaving and subsiding of the ground, as this disparity drops to 21 days in areas of Niyaqu basin where R^2 >0.9 and rises to 29 where R^2 <0.6. The high disparity between the DMS results of ascending and descending data sets and the high shift error of the sine function suggest that the sinusoidal HSM does not produce reliable results of the DMS for such a short time series with only 3 to 4 seasons.

6.3 Multiannual displacements in steep terrain

Most data points on slopes in both basins show downslope velocities of 8 to 17 mm yr^{-1} with a small number of landforms moving faster than ~~50~~30 mm yr^{-1}. The instability of most ~~sloped areas~~steep terrain is to be expected, as there is very little deep-rooted vegetation to prevent the unconsolidated material from sliding. ~~Most~~In our field campaigns we observed that soil covered slopes, especially in the Niyaqu basin,~~ heavily~~ feature Kobresia pygmea pastures, which forms a grass mat with a thick root system of up to 30 cm. This may provide some stability in the absence of larger vegetation, however both climate change and overgrazing are degrading this grass mat (Miehe et al., 2008), which could lead to larger sliding velocities in the future.

When studying relatively fast land surface changes with InSAR, it is important to consider the maximum LOS displacement that can be calculated reliably between two SAR acquisitions. Among other factors this is dependent on the wavelength of the satellite (5.6 cm for Sentinel-1) and the temporal baseline of the interferogram. Measurements of displacement exceeding a quarter of the wavelength between two acquisitions are unreliable (Crosetto et al., 2016) and are likely to lead to an underestimation of the displacement signal and low coherence values. This is the case for some of our fast moving landforms during the summers of 2016, when the temporal baseline is up to 96 days for the Qugaqie basin in descending orbit. It is therefore likely that we underestimate velocities during that time period. Most interferograms feature much shorter baselines of 12 to 36 days and are therefore not affected by this issue. It is unlikely that this is the cause of the linear pattern of the fastest landforms, as the temporal baselines of the summer of 2018 are short and also do not show a clear acceleration of the velocity (Fig. 6B). The high velocity reduces coherence values in in the center of the fastest landforms and leads to decorrelation in some cases.

6.4 Seasonal displacements in steep

Most slopes moving at least 10 mm yr^{-1} experience a clear seasonal displacement signal, with velocities increasing ~~significantly during~~considerably towards the end of the summer monsoon period (Fig. 6C). Monsoon season is associated with both the highest temperatures and approximately 80 % of the annual precipitation over a period of 4 months from June to September (NAMORS, 2018). For Qugaqie basin it is also the only time when the average daily air temperature exceeds 0°C (Zhang et al., 2013). ~~Relatively warm temperatures thaw the ground, likely~~ The clear connection between accelerated ~~by~~ surface displacement and the increased ~~thermal conductivity~~air temperature in summer make freeze-thaw related processes like solifluction a likely driver of ~~moist~~displacements on soil ~~compared~~covered slopes. Solifluction describes a process where seasonal freezing and thawing of the ground induces downslope displacement of up to ~~dry soil (Li et al., 2015), which facilitates faster sliding during this period.~~ 1 m yr^{-1} (Matsuoka, 2001). Affected slopes in the Qugaqie basin display downslope velocities of mostly 50 to 150 mm yr^{-1} and up to 400 mm yr^{-1} in some cases towards the end of the summer season.

Remarkably we do not observe this ~~seasonal velocity~~seasonally accelerated pattern for most of the fastest moving landforms like rock glaciers. These landforms are ~~sliding~~creeping at ~~very~~comparatively linear rates, without ~~significant~~distinct differences between summer and winter (Fig. 6B), often with multiannual downslope velocities >50 mm yr^{-1}. We were able to identify 19 of these landforms in the Niyaqu basin and ~~32~~33 in the Qugaqie basin by ~~clustering~~forming clusters of data points with a ~~strong~~ linear velocity pattern (less than 50% acceleration of the velocity in summer) and ~~high~~ slope velocities >50 mm yr^{-1}. Our spatial data coverage of steep slopes is better in the Qugaqie basin compared to the Niyaqu basin. It is therefore unlikely that this 19 to ~~32~~33 comparison is an accurate reflection of the difference in frequency of these landforms between both study areas. ~~We see it however as a strong indication of a landform relegated exclusively to mountainous terrain. It is possible~~It is likely that some of these clusters have been misidentified as linearly moving, while actually featuring both the seasonal ~~freeze-thaw~~heave-subsidence cycle prevalent in the valleys and the seasonal sliding pattern of the slopes. In some cases those two cycles may cancel each other out to such a degree that the resulting velocity appears linear. This can be observed at the interface between slopes and the valley (Fig. ~~3C).~~ 7A/B).

We determined from optical satellite data, DEM analysis and field observations, that ~~some~~36 % of these linearly creeping clusters are associated with rock glaciers or ~~other periglacial landforms, whose~~protalus ramparts, where motion is driven by ~~high~~massive ice ~~content.~~within the landforms (Whalley and Azizi, 2003). It is therefore possible that fast linear velocity is an indicator for ice-driven landforms. This disagrees with some other studies observing strong seasonal variations in the velocities of rock glaciers (e.g. Kääb and Vollmer, 2000). Rock glacier kinematics are highly dependent on the climatic setting, ice content, ground lithology and slope (Haeberli et al., 2006), making comparison between rock glaciers of different regions difficult. Rock glaciers studied in ~~the Himalaya in~~ north-western Bhutan show velocities of up to 300 mm yr^{-1} and in rare cases up to 700 mm yr^{-1} (Dini et al., 2019~~) and in the Khumbu Himalaya (Barsch and Jakob, 1998) show comparable rock glacier velocities of 18 to 35 and 100 to 200 mm yr-1 respectively.~~). However, ~~Dini et al. (2019) did not project their data along the steepest slope, which explains the lower values, and~~ neither study ~~analyzed~~could analyze the seasonal displacement patterns of rock glaciers ~~in their study area. We can therefore not be certain if fast linear motion is indeed an indicator~~due to large temporal baselines of ~~ice-driven motion~~their interferograms. Strozzi et al. (2020) observe rock glacier velocities of approximately 1.5 to 2 m yr^{-1} in the Argentinian Andes, 2 to 4 m yr^{-1} in Western Greenland and 1 to 2 m yr^{-1} in ~~our study areas or if the linearity of the motion is related to other processes. Further field work~~the Swiss Alps. The former two show a velocity increase of ~~permafrost and subsurface ice distribution in Qugaqie basin and neighboring regions is required to corroborate or disprove this hypothesis~~30 to 50 % and the latter around 100 % between winter and late summer.

Not all fast and linearly moving areas are associated with landforms containing massive ice. Rock slope instabilities such as rock slides are common on the debris covered slopes and while most of them follow a seasonally accelerated displacement pattern, around 24 % of fast and linearly moving areas are likely associated with rock slope instabilities. We can therefore not be certain if fast linear motion is indeed an indicator of displacement driven by massive ice. Their relatively low dependency on seasonality indicates however, that their displacement is mainly gravity-driven as opposed to slopes with strong seasonal variations, where the displacement is driven by both gravity and freeze-thaw related processes.

7 Conclusion

We clearly observe ~~clearly~~ both multiannual and seasonal surface displacement patterns ~~at lake~~in the Nam Co area. Most flat areas are relatively stable on a multiannual scale but show a strong seasonal pattern induced by ~~thawing~~ freezing of the active layer in ~~spring and summer and its subsequent freezing in~~ late autumn and winter~~.~~ and its subsequent thawing in spring and summer. This ~~causes~~induces a vertical oscillation with an amplitude of 5 to 10 mm in most regions with areas near water bodies showing a more pronounced pattern with an amplitude of up to 24 mm. ~~We observe uplift rates of 10 to 40 mm yr-1 in near some rivers, likely representing accumulation of material, and subsidence rates of 10 to 20 mm yr-1, which may be associated with permafrost degradation. Slopes in both study areas are largely~~Most steep terrain in both study areas are unstable, due to the unconsolidated material and the lack of deep-rooted vegetation. They move downslope with velocities of 8 to 17 mm yr^{-1}. Most ~~slopes follow~~steep terrain shows a seasonal ~~sliding~~displacement pattern~~, forced by the monsoonal climate, which brings both heavy rainfall~~ driven by freeze-thaw processes on soil covered slopes and ~~warmer temperatures~~associated with rock slope instabilities on debris covered slopes. Downslope velocities on these slopes accelerate from around 20 mm yr^{-1} in winter to ~~an otherwise cold and dry region. Velocities may be up~~50 to ~~one magnitude larger~~150 mm yr^{-1} to in late summer ~~compared to winter, with some slopes in the Qugaqie basin arresting almost all motion during the winter months.~~for mean velocities of 30 to 70 mm yr^{-1}. The fastest ~~moving~~ landforms can reach ~~downslope~~mean velocities of ~~over~~ 100 to 180 mm yr^{-1}. These landforms do not follow the ~~seasonal~~seasonally accelerated sliding pattern of most slopes but creep linearly with ~~very~~ little difference between summer and winter velocity~~.~~ indicating that they are not related to freeze-thaw processes. While we have identified some of those landforms as rock glaciers and protalus ramparts, we cannot be certain ~~if~~to which extent fast linear velocity is an indicator for ~~ice~~ motion driven ~~motion~~ by massive ice in this area. ~~Further field work is necessary to corroborate or disprove this hypothesis.~~

Data availability

https://doi.pangaea.de/10.1594/PANGAEA.907743

Team List

M. Sc. Eike Reinosch, Institute of Geodesy and Photogrammetry, Technische Universität Braunschweig, 38106, Braunschweig, Germany, e.reinosch@tu-braunschweig.de, phone: +49 531 391 94587

M. Sc. Johannes Buckel, Institute of Geophysics and extraterrestrial Physics, Technische Universität Braunschweig, 38106, Braunschweig, Germany, j.buckel@tu-bs.de, phone: +49 531 391 8506

Dr. Jie Dong, School of Remote Sensing and Information Engineering, Wuhan University, 430079, Wuhan, China, dongjie@whu.edu.cn, phone: +86 15072317889

Prof. Markus Gerke, Institute of Geodesy and Photogrammetry, Technische Universität Braunschweig, 38106, Braunschweig, Germany, m.gerke@tu-bs.de, phone: +49 531 391 94570

Dr. Jussi Baade, Department of Geography, Friedrich-Schiller- Universität Jena, 07743, Jena, Germany, jussi.baade@uni-jena.de, phone: +49 3641 9-48803

Dr. Björn Riedel, Institute of Geodesy and Photogrammetry, Technische Universität Braunschweig, 38106, Braunschweig, Germany, b.riedel@tu-bs.de, phone: +49 531 391 94593

Author Contribution

The majority of the scientific writing and the figures were produced by Eike Reinosch. He also performed most of the literature research and data processing. Johannes Buckel performed literature research of the study areas, especially about their geomorphology, and wrote parts of the respective section. Furthermore he proof read the entire document regarding geomorphological and geological data and established connections between the results of the satellite analysis and relevant geomorphological landforms and processes in the field. Dr. Björn Riedel provided guidance regarding InSAR processing and proof reading of the manuscript, with a focus on the technical aspects of InSAR time series analysis. He also secured the funding for this research as part of the TransTiP project. Prof. Markus Gerke proof read the manuscript, provided guidance about the relevant research questions, research direction and the manuscript structure and aided in establishing connections to other remote sensing instituting to discuss the content of this research with fellow researchers. Dr. Jussi Baade secured funding for the project, evaluated potential study areas and provided us with additional data through additional proposals to the DLR. Dr. Jie Dong performed a review of the methods used with a focus on the seasonal displacement signal present in our data and the potential causes thereof.

Competing Interests

The authors declare that they have no conflict of interests.

Acknowledgements

We would like to thank the DLR for providing us with the high-resolution TanDEM-X DEM for our data processing (Proposal ID DEM_HYDR1727) and the ESA and Copernicus for making Sentinel-1 and Sentinel-2 data freely available to the public. We are especially grateful to the 'Deutsche Forschungsgemeinschaft' (DFG) for funding our work as part of the Sino-German project 'Geo-ecosystems in transition on the Tibetan Plateau' (TransTiP; GRK 2309/1). We thank our Chinese colleagues, who have worked tirelessly to support us before and during our field work.

References

~~Barsch, D. and Jakob, M.: Mass transport by active rockglaciers in the Khumbu Himalaya. Geomorphology, 26(1-3), 215-222, https://doi.org/10.1016/S0169-555X(98)00060-9, 1998.~~
Antonova, S., Sudhaus, H., Strozzi, T., Zwieback, S., Kääb, A., Heim, B., Langer. M., Bornemann N. and Boike, J.: Thaw subsidence of a Yedoma landscape in northern Siberia, measured in situ and estimated from TerraSAR-X interferometry. Remote Sensing, 10(4), 494, https://doi.org/10.3390/rs10040494, 2018.

Åkerman, H. J. and Johansson, M.: Thawing permafrost and thicker active layers in sub-arctic Sweden. Permafrost and Periglacial Processes, 19(3), 279-292, https://doi.org/10.1002/ppp.626, 2008.

Bateson, L., Cigna, F., Boon, D. and Sowter, A.: The application of the Intermittent SBAS (ISBAS) InSAR method to the South Wales Coalfield, UK. International Journal of Applied Earth Observation and Geoinformation, 34, 249-257, https://doi.org/10.1016/j.jag.2014.08.018, 2015.

Bauer, A., Paar, G. and Kaufmann, V.: Terrestrial laser scanning for rock glacier monitoring. In 8th International Conference on Permafrost, Proceedings (Vol. 1, pp. 55-60), 2003.

Berardino, P., Fornaro, G., Lanari, R., and Sansosti, E.: A new algorithm for surface deformation monitoring based on small baseline differential SAR interferograms. IEEE Transactions on geoscience and remote sensing, 40(11), 2375-2383, https://doi.org/10.1109/TGRS.2002.803792, 2002.

Bolch, T., Yao, T., Kang, S., Buchroithner, M. F., Scherer, D., Maussion, F., Huintjes, E., and Schneider, C.: A glacier inventory for the western Nyainqentanglha Range and the Nam Co Basin, Tibet, and glacier changes 1976–2009, The Cryosphere, 4, 419–433, https://doi.org/10.5194/tc-4-419-2010, 2010.

Crosetto, M., Monserrat, O., Cuevas-González, M., Devanthéry, N. and Crippa, B.: Persistent scatterer interferometry: A review. ISPRS Journal of Photogrammetry and Remote Sensing, 115, 78-89, https://doi.org/10.1016/j.isprsjprs.2015.10.011, 2016.

Daanen, R. P., Grosse, G., Darrow, M. M., Hamilton, T. D. and Jones, B. M.: Rapid movement of frozen debris-lobes: implications for permafrost degradation and slope instability in the south-central Brooks Range, Alaska. Natural Hazards and Earth System Sciences, 12(5), 1521-1537, https://doi.org/10.5194/nhess-12-1521-2012, 2012.

Daout, S., Doin, M. P., Peltzer, G., Socquet, A. and Lasserre, C.: Large-scale InSAR monitoring of permafrost freeze-thaw cycles on the Tibetan Plateau. Geophysical Research Letters, 44(2), 901-909, https://doi.org/10.1002/2016GL070781, 2017.

Dini, B., Daout, S., Manconi, A. and Loew, S.: ~~Investigation~~Classification of slope ~~instabilities in NW Bhutan as derived from systematic~~processes based on multitemporal DInSAR analyses~~. Engineering Geology, 259, 105111, https://doi.org/10.1016/j.enggeo.2019.04.008, 2019.~~ in the Himalaya of NW Bhutan. Remote Sensing of Environment, 233, 111408, https://doi.org/10.1016/j.rse.2019.111408, 2019.

Dong, J., Zhang, L., Liao, M. and Gong, J.: Improved correction of seasonal tropospheric delay in InSAR observations for landslide deformation monitoring. Remote Sensing of Environment, 233, 111370, https://doi.org/10.1016/j.rse.2019.111370, 2019.

ESA (European Space Agency): SENTINEL-1. ESA's Radar Observatory Mission for GMES Operational Services, ESA SP-1322/1, Noordwijk, 2012.

Eriksen, H. Ø., Lauknes, T. R., Larsen, Y., Corner, G. D., Bergh, S. G., Dehls, J. and Kierulf, H. P.: Visualizing and interpreting surface displacement patterns on unstable slopes using multi-geometry satellite SAR interferometry (2D InSAR). Remote Sensing of Environment, 191, 297-312, https://doi.org/10.1016/j.rse.2016.12.024, 2017.

Fischer, L., Kääb, A., Huggel, C. and Noetzli, J.: Geology, glacier retreat and permafrost degradation as controlling factors of slope instabilities in a high-mountain rock wall: the Monte Rosa east face. Natural Hazards and Earth System Sciences, 6(5), 761-772, https://doi.org/10.5167/uzh-20217, 2006.

Fort, F. and van Vliet-Lanoe, B.: Permafrost and periglacial environment of Western Tibet. Landform Analysis, 5, 25-29, 2007.

French, H. M.: The periglacial environment. Fourth Edition. John Wiley & Sons, Chichester, England, 2017.

Haeberli, W., Hallet, B., Arenson, L., Elconin, R., Humlum, O., Kääb, A., Kaufmann, V., Ladanyi, B., Matsuoka, N., Springmann, S. and Mühll, D. V.: Permafrost creep and rock glacier dynamics. Permafrost and Periglacial Processes, 17(3), 189-214, https://doi.org/10.1002/ppp.561, 2006.

Jarvis, A., Reuter, H. I., Nelson, A. and Guevara, E.: Hole-filled SRTM for the globe Version 4, International Centre for Tropical Agriculture (CIAT), available from http://srtm.csi.cgiar.org, 2008.

Jiang, L., Nielsen, K., Andersen, O. B. and Bauer-Gottwein, P.: Monitoring recent lake level variations on the Tibetan Plateau using CryoSat-2 SARIn mode data. Journal of Hydrology, 544, 109-124, https://doi.org/10.1016/j.jhydrol.2016.11.024, 2017.

Jones, D. B., Harrison, S., Anderson, K. and Whalley, W. B.: Rock glaciers and mountain hydrology: A review. Earth-Science Reviews, https://doi.org/10.1016/j.earscirev.2019.04.001, 2019.

Joshi, N., Baumann, M., Ehammer, A., Fensholt, R., Grogan, K., Hostert, P., Jepsen, R. J., Kuemmerle, T., Meyfroidt, P., Mitchard, E. T. A., Reiche, J. Ryan, C. M. and Waske, B.: A review of the application of optical and radar remote sensing data fusion to land use mapping and monitoring. Remote Sensing, 8(1), 70, https://doi.org/10.3390/rs8010070, 2016.

Kääb, A.: Remote sensing of permafrost-related problems and hazards. Permafrost and periglacial processes, 19(2), 107-136, https://doi.org/10.1002/ppp.619, 2008.

Kapp, J. L. D. A., Harrison, T. M., Kapp, P., Grove, M., Lovera, O. M. and Lin, D.: Nyainqentanglha Shan: a window into the tectonic, thermal, and geochemical evolution of the Lhasa block, southern Tibet. Journal of Geophysical Research: Solid Earth, 110(B8), https://doi.org/10.1029/2004JB003330, 2005.

Keil, A., Berking, J., Mügler, I., Schütt, B., Schwalb, A. and Steeb, P.: Hydrological and geomorphological basin and catchment characteristics of Lake Nam Co, South-Central Tibet. Quaternary International, 218(1-2), 118-130, https://doi.org/10.1016/j.quaint.2009.02.022, 2010.

Kneisel, C., Rödder, T. and Schwindt, D.: Frozen ground dynamics resolved by multi-year and year-round electrical resistivity monitoring at three alpine sites in the Swiss Alps. Near Surface Geophysics, 12(1), 117-132, https://doi.org/10.3997/1873-0604.2013067, 2014.

Kropáček, J., Braun, A., Kang, S., Feng, C., Ye, Q. and Hochschild, V.: Analysis of lake level changes in Nam Co in central Tibet utilizing synergistic satellite altimetry and optical imagery. International Journal of Applied Earth Observation and Geoinformation, 17, 3-11, https://doi.org/10.1016/j.jag.2011.10.001, 2012.

Lei, Y., Yao, T., Bird, B. W., Yang, K., Zhai, J. and Sheng, Y.: Coherent lake growth on the central Tibetan Plateau since the 1970s: Characterization and attribution. Journal of Hydrology, 483, 61-67, https://doi.org/10.1016/j.jhydrol.2013.01.003, 2013.

Li, Z. W., Xu, W. B., Feng, G. C., Hu, J., Wang, C. C., Ding, X. L. and Zhu, J. J.: Correcting atmospheric effects on InSAR with MERIS water vapour data and elevation-dependent interpolation model. Geophysical Journal International, 189(2), 898-910, https://doi.org/10.1111/j.1365-246X.2012.05432.x, 2012.

Li, B., Yu, Z., Liang, Z. and Acharya, K.: Hydrologic response of a high altitude glacierized basin in the central Tibetan Plateau. Global and Planetary Change, 118, 69-84, https://doi.org/10.1016/j.gloplacha.2014.04.006, 2014.

Li, Z., Zhao, R., Hu, J., Wen, L., Feng, G., Zhang, Z. and Wang, Q.: InSAR analysis of surface deformation over permafrost to estimate active layer thickness based on one-dimensional heat transfer model of soils. Scientific Reports, 5, 15542, https://doi.org/10.1038/srep15542, 2015.

Li, Q.: Spatial variability and long-term change in pollen diversity in Nam Co catchment (central Tibetan Plateau): Implications for alpine vegetation restoration from a paleoecological perspective. Science China Earth Sciences, 61(3), 270-284, https://doi.org/10.1007/s11430-017-9133-0, 2018.

Liu, L., Millar, C. I., Westfall, R. D. and Zebker, H.: Surface motion of active rock glaciers in the Sierra Nevada, California, USA: inventory and a case study using InSAR. The Cryosphere. 7: 1109-1119, 7, 1109-1119, https://doi.org/10.5194/tc-7-1109-2013, 2013.

Matsuoka, N., Abe, M. and Ijiri, M.: Differential frost heave and sorted patterned ground: field measurements and a laboratory experiment. Geomorphology, 52(1-2), 73-85, https://doi.org/10.1016/S0169-555X(02)00249-0, 2003.

Matsuoka, N.: Solifluction rates, processes and landforms: a global review. Earth-Science Reviews, 55(1-2), 107-134, https://doi.org/10.1016/S0012-8252(01)00057-5, 2001.

McKenzie, J. M. and Voss, C. I.: Permafrost thaw in a nested groundwater-flow system. Hydrogeology Journal, 21(1), 299-316, http://dx.doi.org/10.1007%2Fs10040-012-0942-3, 2013.

Messerli, B., Viviroli, D., and Weingartner, R.: Mountains of the World: Vulnerable Water Towers for the 21st Century. AMBIO, 2004, 29-3, 2004.

Miehe, G., Miehe, S., Kaiser, K., Jianquan, L. and Zhao, X.: Status and dynamics of the Kobresia pygmaea ecosystem on the Tibetan Plateau. AMBIO: A Journal of the Human Environment, 37(4), 272-280, https://doi.org/10.1579/0044-7447(2008)37[272:SADOTK]2.0.CO;2, 2008.

~~Mügler, I., Gleixner, G., Günther, F., Mäusbacher, R., Daut, G., Schütt, B., Berking, J., Schwalb, A., Schwark, L., Xu, B., Yao, T., Zhu,~~Müller, J., Vieli, A. and Gärtner-Roer, I.: Rock glaciers on the run-understanding rock glacier landform evolution and recent changes from numerical flow modeling. The Cryosphere, 10(6), 2865-2886, https://doi.org/10.5194/tc-10-2865-2016, 2016.

~~L. and Yi, C.: A multi-proxy approach to reconstruct hydrological changes and Holocene climate development of Nam Co, Central Tibet. Journal of Paleolimnology, 43(4), 625-648, https://doi.org/10.1007/s10933-009-9357-0, 2010.~~

NAMORS 2018: Meteorological Data for the NAMORS research station, 2010 to 2017. ITP – CAS Lhasa

Notti, D., Herrera, G., Bianchini, S., Meisina, C., García-Davalillo, J. C. and Zucca, F.: A methodology for improving landslide PSI data analysis. International Journal of Remote Sensing, 35(6), 2186-2214, https://doi.org/10.1080/01431161.2014.889864, 2014.

Osmanoğlu, B., Sunar, F., Wdowinski, S. and Cabral-Cano, E.: Time series analysis of InSAR data: Methods and trends. ISPRS Journal of Photogrammetry and Remote Sensing, 115, 90-102, https://doi.org/10.1016/j.isprsjprs.2015.10.003, 2016.

Riseborough, D., Shiklomanov, N., Etzelmüller, B., Gruber, S. and Marchenko, S.: Recent advances in permafrost modelling. Permafrost and Periglacial Processes, 19(2), 137-156, dx.doi.org/10.1002/ppp.615, 2008.

Rouyet, L., Lauknes, T. R., Christiansen, H. H., Strand, S. M. and Larsen, Y.: Seasonal dynamics of a permafrost landscape, Adventdalen, Svalbard, investigated by InSAR. Remote Sensing of Environment, 231, 111236, https://doi.org/10.1016/j.rse.2019.111236, 2019.

Schuur, E. A., McGuire, A. D., Schädel, C., Grosse, G., Harden, J. W., Hayes, D. J., Hugelius, G., Koven, C. D., Kuhry, P., Lawrence, D. M., Natali, S. M., Olefeldt, D., Romanovsky, V. E., Schaefer, K., Turetsky, M. R., Treat, C. C. and Vonk, J. E.: Climate change and the permafrost carbon feedback. Nature, 520(7546), 171-179, https://doi.org/10.1038/nature14338, 2015.

Shur, Y., Hinkel, K. M. and Nelson, F. E.: The transient layer: implications for geocryology and climate-change science. Permafrost and Periglacial Processes, 16(1), 5-17, https://doi.org/10.1002/ppp.518, 2005.

Song, C., Huang, B., Ke, L. and Richards, K. S.: Seasonal and abrupt changes in the water level of closed lakes on the Tibetan Plateau and implications for climate impacts. Journal of Hydrology, 514, 131-144, https://doi.org/10.1016/j.jhydrol.2014.04.018, 2014.

Sowter, A., Bateson, L., Strange, P., Ambrose, K. and Syafiudin, M. F.: DInSAR estimation of land motion using intermittent coherence with application to the South Derbyshire and Leicestershire coalfields. Remote Sensing Letters, 4(10), 979-987, https://doi.org/10.1080/2150704X.2013.823673, 2013.

Strozzi, T., Caduff, R., Jones, N., Barboux, C., Delaloye, R., Bodin, X., Kääb, A., Mätzler, E. and Schrott, L.: Monitoring Rock Glacier Kinematics with Satellite Synthetic Aperture Radar. Remote Sensing, 12(3), 559, https://doi.org/10.3390/rs12030559, 2020.

Tian, K., Liu, J., Kang, S., Campbell, I. B., Zhang, F., Zhang, Q. and Lu, W.: Hydrothermal pattern of frozen soil in Nam Co lake basin, the Tibetan Plateau. Environmental Geology, 57(8), 1775-1784, https://doi.org/0.1007/s00254-008-1462-2, 2009.

~~Wang, K., Wang, P., Liu, J., Sparrow, M., Haginoya, S. and Zhou, X. (2005). Variation of surface albedo and soil thermal parameters with soil moisture content at a semi-desert site on the western Tibetan Plateau. Boundary-Layer Meteorology, 116(1), 117-129, https://doi.org/10.1007/s10546-004-7403-z, 2005.~~

Wang, X., Liu, L., Zhao, L., Wu, T., Li, Z., and Liu, G.: Mapping and inventorying active rock glaciers in the northern Tien Shan of China using satellite SAR interferometry, The Cryosphere, 11, 997–1014, https://doi.org/10.5194/tc-11-997-2017, 2017.

Wessel, B., Huber, M., Christian Wohlfart, C., Ursula Marschalk, U., Detlev Kosmann, D., and Achim Roth, A.: Accuracy assessment of the global TanDEM-X Digital Elevation Model with GPS data, ISPRS Journal of Photogrammetry and Remote Sensing, 139, 171-182, https://doi.org/10.1016/j.isprsjprs.2018.02.017, 2018.

Whalley, W. B. and Azizi, F.: Rock glaciers and protalus landforms: Analogous forms and ice sources on Earth and Mars. Journal of Geophysical Research: Planets, 108(E4), https://doi.org/10.1029/2002JE001864, 2003.

Wu, Q., Zhang, T. and Liu, Y.: Permafrost temperatures and thickness on the Qinghai-Tibet Plateau. Global and Planetary Change, 72(1-2), 32-38, https://doi.org/10.1016/j.gloplacha.2010.03.001, 2010.

Yagüe-Martínez, N., Prats-Iraola, P., Gonzalez, F. R., Brcic, R., Shau, R., Geudtner, D., Eineder, M. and Bamler, R.: Interferometric processing of Sentinel-1 TOPS data. IEEE Transactions on Geoscience and Remote Sensing, 54(4), 2220-2234, https://doi.org/10.1109/TGRS.2015.2497902, 2016.

Yao, T., Liu, X., Wang, N. and Shi, Y.: Amplitude of climatic changes in Qinghai-Tibetan Plateau. Chinese Science Bulletin, 45(13), 1236-1243, https://doi.org/10.1007/BF02886087, 2000.

Yao, T., Pu, J., Lu, A., Wang, Y. and Yu, W.: Recent glacial retreat and its impact on hydrological processes on the Tibetan Plateau, China, and surrounding regions. Arctic, Antarctic, and Alpine Research, 39(4), 642-650, https://doi.org/10.1657/1523-0430(07-510)[YAO]2.0.CO;2, 2007.

Yao, T., Masson-Delmotte, V., Gao, J., Yu, W., Yang, X., Risi, C., Sturm, C., Werner, M., Zhao, H., He, Y., Ren, W., Tian, L., Shi, C. and Hou, S.: A review of climatic controls on δ18O in precipitation over the Tibetan Plateau: Observations and simulations. Reviews of Geophysics, 51(4), 525-548, https://doi.org/10.1002/rog.20023, 2013.

Ye, Q., Zong, J., Tian, L., Cogley, J. G., Song, C. and Guo, W.: Glacier changes on the Tibetan Plateau derived from Landsat imagery: mid-1970s–2000–13. Journal of Glaciology, 63(238), 273-287, https://doi.org/10.1017/jog.2016.137, 2017.

Yu, Z., Wu, G., Keys, L., Li, F., Yan, N., Qu, D. and Liu, X.: Seasonal variation of chemical weathering and its controlling factors in two alpine catchments, Nam Co basin, central Tibetan Plateau. Journal of Hydrology, 576, 381-395, https://doi.org/10.1016/j.jhydrol.2019.06.042, 2019.

Zhang, G., Kang, S., Fujita, K., Huintjes, E., Xu, J., Yamazaki, T., Haginoya, S., Wei, Y., Scherer, D., Schneider, C. and Yao, T.: Energy and mass balance of Zhadang glacier surface, central Tibetan Plateau. Journal of Glaciology, 59(213), 137-148, https://doi.org/10.3189/2013JoG12J152, 2013.

Zhang, Y., and Michalowski, R. L.: Thermal-hydro-mechanical analysis of frost heave and thaw settlement. Journal of geotechnical and geoenvironmental engineering, 141(7), 04015027, https://doi.org/10.1061/(ASCE)GT.1943-5606.0001305, 2015.

Zhang, G., Li, J. and Zheng, G.: Lake-area mapping in the Tibetan Plateau: an evaluation of data and methods. International Journal of Remote Sensing, 38(3), 742-772, https://doi.org/10.1080/01431161.2016.1271478, 2017.

Zhao, R., Li, Z. W., Feng, G. C., Wang, Q. J. and Hu, J.: Monitoring surface deformation over permafrost with an improved SBAS-InSAR algorithm: With emphasis on climatic factors modeling. Remote Sensing of Environment, 184, 276-287, https://doi.org/10.1016/j.rse.2016.07.019, 2016.

Zhou, S., Kang, S., Chen, F. and Joswiak, D. R.: Water balance observations reveal significant subsurface water seepage from Lake Nam Co, south-central Tibetan Plateau. Journal of Hydrology, 491, 89-99, https://doi.org/10.1016/j.jhydrol.2013.03.030, 2013.

Zink, M., Bachmann, M., Bräutigam, B., Fritz, T., Hajnsek, I., Moreira, A., Wessel, B., and Krieger, G.: TanDEM-X: The New Global DEM Takes Shape, IEEE Geoscience and Remote Sensing Magazin, 2(2), 8 – 23, https://doi.org/10.1109/MGRS.2014.2318895, 2014.

Zou, D., Zhao, L., Yu, S., Chen, J., Hu, G., Wu, T., Wu, J., Xie, C., Wu, X., Pang, Q., Wang, W., Du, E., Li, W., Liu, G., Li, J., Qin, Y., Qiao, Y., Wang, Z., Shi, J. and Cheng, G.: A new map of permafrost distribution on the Tibetan Plateau. The Cryosphere, 11(6), 2527, https://doi.org/10.5194/tc-11-2527-2017, 2017.

Zwieback, S., Hensley, S., and Hajnsek, I.: Soil moisture estimation using differential radar interferometry: Toward separating soil moisture and displacements. IEEE Transactions on Geoscience and Remote Sensing, 55(9), 5069-5083, https://doi.org/10.1109/TGRS.2017.2702099, 2017.